

Ocean Dynamics and the Carbon Cycle

Principles and Mechanisms

Richard G. Williams
Michael J. Follows

CAMBRIDGE

Biological fundamentals

The ocean is teeming with life. In sunlit surface waters, every millilitre may contain hundreds of thousands of phytoplankton (Fig. 5.1a). These tiny plants, some as small as a micron, use chlorophyll to capture energy from sunlight to create the organic molecules that make up their bodies and fuel the biochemical reactions that support almost all marine life. While most individual phytoplankton cells are invisible to the naked eye, collectively their chlorophyll colours the water. If you take a cruise from the tropics to the high latitude oceans, the surface waters turn from a clear blue to an opaque greenish tinge. This change in colour reflects how the abundance of phytoplankton increases with the availability of essential nutrients, sunlight, temperature and the predators which eat them.

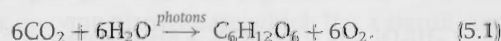
Phytoplankton are at the bottom of the food chain: they create fresh organic matter from dissolved nutrients, carbon dioxide, and energy from sunlight. Many of the phytoplankton are eaten by other plankton (Fig. 5.1a) which in turn are consumed by larger organisms, ultimately sustaining large fish and mammals at the top of the food chain. Eventually some of the organic matter sinks to the deeper, dark waters either as dead cells or faecal pellets. This organic matter is utilised by a host of organisms, including bacteria, which recover the last of the energy originally captured by the phytoplankton and, in the process of respiration, convert organic molecules back to inorganic form.

In this chapter, we discuss the biological processes which are particularly relevant to the marine carbon cycle, as depicted in Fig. 5.1b. We

begin at the scale of molecules and individual living cells, describing some fundamental aspects of biochemical reactions, cellular composition and physiology. We discuss how phytoplankton populations acquire the nutrients and light they need to create new organic molecules, as well as the variety of strategies which allows them to thrive in diverse environments. We address where organic carbon is formed in the open ocean and its subsequent fate in surface and deep waters, and finally discuss how slight differences in the biological role and processing of nutrient elements affects their utilisation and distributions over the ocean.

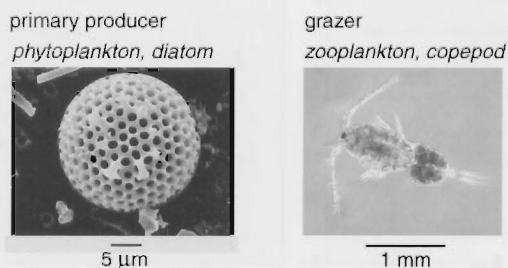
5.1 Photosynthesis and respiration

In a simple view, photosynthesis is the conversion of electromagnetic energy into chemical energy through the formation of organic molecules (Fig. 5.1b). A simple, schematic representation of this process is a chemical reaction where carbon dioxide and water are converted to glucose, $C_6H_{12}O_6$, and molecular oxygen, using energy from photons:

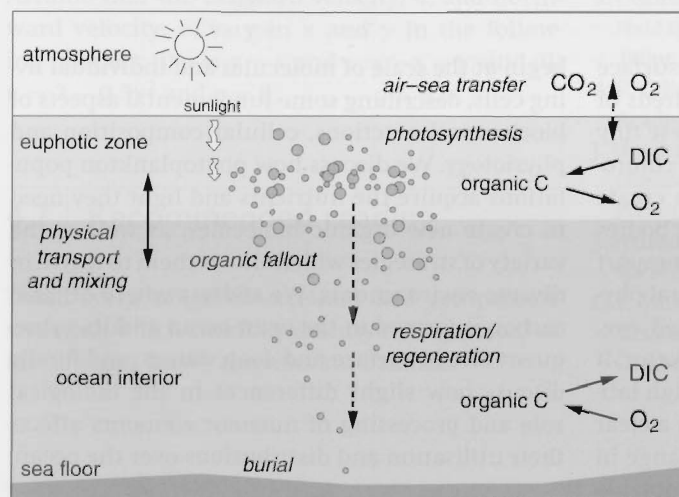


The creation of organic matter from inorganic compounds is called **primary production**. The primary producers in the ocean are phytoplankton, single cells or colonies of cells living freely in the water column. Organisms which make a living by photosynthesis are called **phototrophs**.

(a) marine plankton

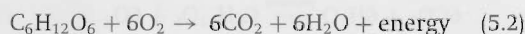


(b) carbon pathways in the ecosystem



The energy for photosynthesis comes from the absorption of visible wavelengths of light. Electromagnetic radiation is rapidly absorbed in seawater; even in very clear water the downward flux of light decays exponentially with depth, limiting viable phytoplankton growth to within typically 200 m of the surface. This region where photosynthesis is viable is called the euphotic layer.

Respiration, the oxidation of organic matter, is the reverse of photosynthesis (Fig. 5.1b). Oxygen is consumed and energy released to fuel biochemical reactions and mechanical work:



Organisms which obtain energy exclusively by harvesting and respiring live or dead organic matter are called heterotrophs. In the ocean they include submicron-scale bacteria, zooplankton preying on phytoplankton, bacteria and smaller zooplankton, as well as fish. Mixotrophs are organisms which adopt both strategies, obtaining

energy and essential elements both by photosynthesis and the harvesting and respiration of existing organic matter.

Figure 5.1 (a) Examples of marine plankton: phytoplankton, the plants of the ocean, are single cells or colonies ranging from about one to 100s of microns in cell size. Copepods are larger zooplankton, typically on the order of a millimetre or more in size, which graze on phytoplankton, bacteria and smaller zooplankton. (b) Photosynthesis by phytoplankton occurs in the sunlit, surface waters, producing organic matter and oxygen. Much of the organic matter is respired back to inorganic form within the euphotic zone, but a significant fraction is transported down, or sinks gravitationally into the deep ocean. Respiration by zooplankton, bacteria and archaea returns the organic material to inorganic forms, including dissolved inorganic carbon. Diatom image courtesy of Zoe Finkel.

5.2 What are marine microbes made of?

Microbes are those organisms which are too tiny to observe with the naked eye and include phytoplankton and heterotrophic bacteria. In order to reproduce and create new individuals, microbes need to maintain a complex set of biochemical machinery, depicted schematically in Fig. 5.2a,b. All these living microbes are made up of molecules which can be classified into a few broad biochemical categories:

- Carbohydrates, such as glucose, are basic organic molecules composed only of carbon, hydrogen and oxygen (see Table 5.1). They

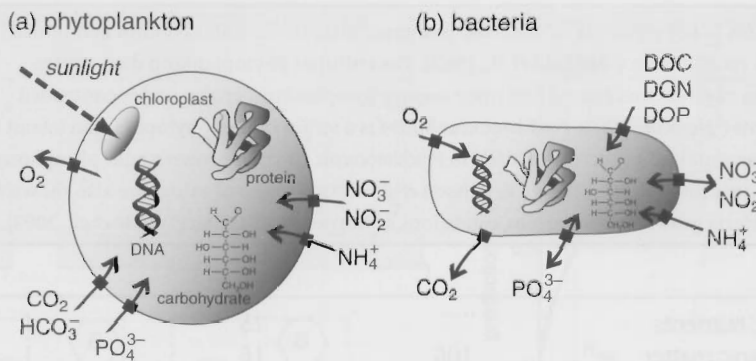


Figure 5.2 Schematic depiction of an idealised (a) phytoplankton, and (b) bacterium. The common physiological demands of resource acquisition and reproduction mean that all microbes manufacture proteins, lipids and nucleic acids. Phytoplankton take up inorganic nutrients, forming carbohydrates by photosynthesis and expelling oxygen as a by-product. Chloroplasts contain the pigments which harvest energy from photons. Bacteria import oxygen and organic matter, acquiring energy through respiration, and return inorganic compounds to the environment.

Table 5.1 Representative biochemical composition of phytoplankton cells: inferred mean molecular composition of major cell components and average contribution to the cell by dry organic weight. Evaluated by Anderson (1995).

Metabolite	Elemental composition	% cell
Protein	$C_{3.83}H_{6.05}O_{1.25}N$	54.4
Carbohydrate	$C_6H_{10}O_5$	25.5
Lipid	$C_{40}H_{74}O_5$	16.1
Nucleic acid	$C_{9.625}H_{12}O_{6.5}N_{3.75}P$	4.0

provide a store of energy and basic building blocks for more complex cellular components.

- Lipids are largely composed of carbon, hydrogen and oxygen, but do incorporate other elements. They provide an energy store and form the basis for important membranes in the cell.
- Proteins provide structural components and perform key functions as enzymes, catalysing the complex biochemical reactions that occur in the cell.
- Nucleic acids are the reproductive machinery of the cell. DNA holds the blueprint of the living organism, while RNA takes that blueprint and creates new proteins, melding together component molecules.

In marine microbes, half of the dry-weight biomass is accounted for by proteins, followed by carbohydrates and lipids, while nucleic acid contributes only a small fraction (Table 5.1).

Each of these components has a different elemental composition, so that most of the cellular nitrogen content is in proteins, while a large fraction of the phosphorus is in nucleic acids (Table 5.1). Trace metals are also incorporated into some proteins, enabling specific enzymatic functions.

5.2.1 How does the elemental composition of microbes vary?

The relative abundance of elements in living cells reflects the abundance and elemental composition of the molecules from which they are composed. There can be significant variations in the biochemical composition of microbial cells within and between species (Table 5.2), even over the lifetime of an individual cell, since cells can alter their biochemical composition as they acclimate or adjust their physiology to cope with a changing environment. For example:

- Some microbes can fix nitrogen, converting nitrogen gas, N_2 , into organic form. They use the enzyme nitrogenase which has a significant iron content, so nitrogen fixers have a high cellular iron quota.
- When cells are growing and dividing rapidly, they produce extra RNA, which transcribes the blueprint of DNA into proteins, increasing their phosphorus content.
- Some phytoplankton maintain an internal store of nutrient elements, acquiring nutrients from

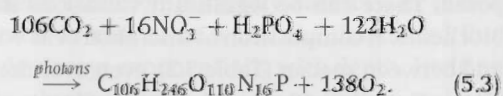
Table 5.2 | The ratios of key elements in dissolved inorganic form in the water column and in marine phytoplankton and zooplankton (^aRedfield *et al.*, 1963). The cultured phytoplankton data are the average of 15 species of estuarine, coastal and open ocean phytoplankton grown under controlled laboratory conditions (^bHo *et al.*, 2003). *Prochlorococcus* MED4 is a strain of tiny phytoplankton (about a micron in scale). Elemental ratios were measured in *Prochlorococcus* cultures grown under phosphorus replete and phosphorus limited conditions (^cBertilsson *et al.*, 2003). Ranges of values are also shown for isolated marine bacteria grown under various conditions of nutrient limitation (^dVrede *et al.*, 2002).

Reservoir	C	N	P
^a Marine inorganic nutrients		15	1
^a Bulk marine organic matter	106	16	1
^b Cultured phytoplankton	147 ± 19	16 ± 2	1 ± 0.2
^c <i>Prochlorococcus</i> MED4 (P-replete)	12 ± 17	21.2 ± 4.5	1
^c <i>Prochlorococcus</i> MED4 (P-limited)	464 ± 28	62.3 ± 14.1	1
^d Marine bacteria	35–178	7–18	1

the environment when they are plentiful, but utilising the store when the environment is depleted.

Redfield ratios

Despite the variations within and between species, there is a general consistency in the elemental composition of bulk marine phytoplankton and zooplankton (Table 5.2). This consistency reflects how all marine plankton utilise some common molecular machinery. Incorporating the contributions of nitrogen and phosphorus, the simple representation of photosynthesis in (5.1) can be extended to



The elemental ratios in the idealised organic molecule formed by photosynthesis, C N P O₂ = 106 16 1 -138, are referred to as the 'Redfield ratio' (Table 5.2), reflecting the bulk measurements of Redfield and colleagues (Redfield *et al.*, 1963). They measured the C N P ratio in marine phytoplankton and zooplankton, and estimated the corresponding oxygen production/consumption ratio, P O₂ = 1 -138, by calculating the requirement to oxidise the organic molecules of the measured composition to CO₂, NO₃⁻ and PO₄³⁻. More recent studies have evaluated the oxygen ratio empirically, finding P O₂ = 1 -170 (Takahashi *et al.*, 1985; Anderson and

Sarmiento, 1994). The mismatch can be explained by assuming a slightly different balance between the major classes of biochemical molecules in the organisms (Anderson, 1995), or by adopting a more complex view of photosynthesis than (5.3).

This view of the elemental composition of organic matter and the effect on ocean biogeochemistry is revisited in Section 5.6. Now consider the chemical reactions in which simple molecules are combined to form complex organic substances.

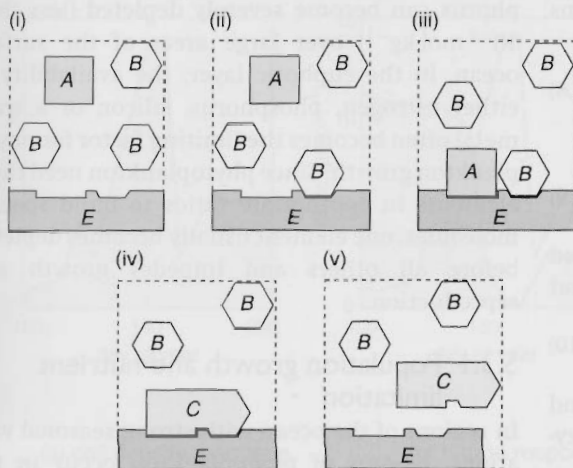
5.2.2 How are organic molecules produced in a cell?

The complex organic molecules of a living cell are the result of chemical reactions between component compounds. The necessary reactions are catalysed by special proteins called enzymes, without which they would proceed very slowly or not at all. While enzymes facilitate reactions, they are not consumed in the process.

Enzymatic reactions can be described as a sequence of stages, as illustrated in Fig. 5.3a:

- Molecules A and B become bound, or complexed, to the enzyme E (panels (i) to (iii)).
- A reaction proceeds between A and B, while attached to the enzyme, forming a product C (panel (iv)).
- The product C is released, freeing the enzyme to repeat the function (panel (v)).

(a) schematic representation of enzyme reactions



(b) mathematical representation

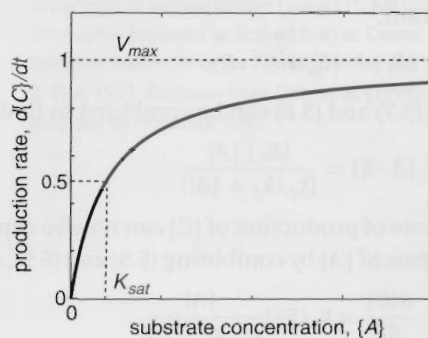
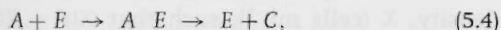


Figure 5.3 Enzymatic reactions: (a) a schematic view, and (b) a mathematical representation. Enzymes are organic molecules which catalyse biochemical reactions, including the production of organic compounds from simpler molecules or substrates. In (a), the enzyme E captures molecules of substrates A and B at receptor sites (i)–(iii), synthesises the product, C (iv) and (v), the product C is released, allowing the enzyme to perform this function again. In (b), the relationship between the rate of production of the product $\{C\}$ and the concentration of $\{A\}$ per unit volume (referred to as a substrate), described by $d\{C\}/dt = V_{max}\{A\}/(K_{sat} + \{A\})$, where V_{max} is the maximum rate of production, and K_{sat} is the half saturation; this relationship follows the Michaelis–Menten model of enzyme reactions.

The Michaelis–Menten model of an enzymatic reaction

Now consider how the simplest form of enzymatic reaction can be represented as a sequence of chemical reactions. Assume that molecules of A are less abundant than B and are limiting the reactions (as depicted in Fig. 5.3a). The sequence of reactions for the molecule A (referred to as a substrate) then follows



where molecule A , becomes bound to a free enzyme, E ; the pair forming a complex, $A E$. Here we consider the simplest case where A does not become detached again. After some time, the complex produces a molecule of the product C , which is released and the enzyme is free to start the cycle again. The two phases are awaiting the ‘arrival’ of the substrate and its subsequent ‘handling’ to form the product.

The rate of production of C from the complex is described by

$$\frac{d\{C\}}{dt} = k_p\{A E\}, \quad (5.5)$$

where curly brackets, $\{C\}$, denote concentration per unit volume (mol m^{-3}) and k_p (s^{-1}) is the rate constant of formation of the product. Usually we are interested in how the rate of formation of product C depends upon the concentration of the substrate, $\{A\}$, rather than $\{A E\}$ as in (5.5). Thus, we need to find the relationship between $\{A\}$ and $\{A E\}$. To make this connection, consider the rate of change of the enzyme–substrate complex, $A E$, in (5.4): this complex increases in concentration when the substrate A binds to the free enzyme E , but decreases in concentration when the product C is formed, which can be written as

$$\frac{d\{A E\}}{dt} = k_f\{A\}\{E\} - k_p\{A E\}, \quad (5.6)$$

where k_f is the rate constant of the forward reaction, $\{A\} + \{E\} \rightarrow \{A E\}$ in units of $(\text{mol m}^{-3})^{-1} \text{s}^{-1}$. If an equilibrium is reached where the amount of complexed enzyme is unchanging, $d\{A E\}/dt = 0$, then

$$\{A E\} = \frac{k_f}{k_p}\{A\}\{E\}. \quad (5.7)$$

If the total enzyme concentration, $\{E_T\}$, defined by the sum of the free and complexed forms, remains constant,

$$\{E_T\} = \{E\} + \{A E\}, \quad (5.8)$$

then (5.7) and (5.8) can be combined to find

$$\{A E\} = \frac{\{E_T\} \{A\}}{(k_p/k_f + \{A\})}. \quad (5.9)$$

The rate of production of $\{C\}$ can now be expressed in terms of $\{A\}$ by combining (5.5) and (5.9), so that

$$\frac{d\{C\}}{dt} = k_p \{E_T\} \frac{\{A\}}{k_p/k_f + \{A\}}, \quad (5.10)$$

where $\{A\}$ appears in both the numerator and denominator on the right-hand side. This enzymatic relation (5.10) is usually re-expressed as

$$\frac{d\{C\}}{dt} = V_{max} \frac{\{A\}}{K_{sat} + \{A\}} \quad (5.11)$$

depicted in Fig. 5.3b, where $V_{max} = k_p \{E_T\}$ (in units of $\text{mol m}^{-3} \text{s}^{-1}$) represents the maximum rate of production which is reached, in theory, when all of the enzyme is constantly in complexed form; and $K_{sat} = k_p/k_f$ (in units of mol m^{-3}) is the half saturation, the substrate concentration at which production is half of that maximum. This form is referred to as Michaelis–Menten kinetics after Michaelis and Menten (1913).

This parameterisation of a two-stage chemical reaction fits empirical data for enzymatic reactions very well. This model turns out to be very relevant for other ecosystem processes including nutrient uptake by cells, light harvesting and predator–prey interactions. Next we consider their relevance for phytoplankton growth.

5.3 How is phytoplankton growth affected by the environment?

What is the relationship between phytoplankton growth and nutrient abundance, light and temperature of the local environment? To grow and reproduce, phytoplankton need light for energy, and dissolved forms of essential elements, including carbon, nitrogen, phosphorus, and trace metals. There is an abundance of dissolved inorganic carbon throughout the ocean, with concentrations typically greater than $1900 \mu\text{mol kg}^{-3}$,

but the inorganic forms of nitrogen and phosphorus can become severely depleted (less than $10^{-9} \text{mol kg}^{-1}$) over large areas of the surface ocean. In the euphotic layer, the availability of either nitrogen, phosphorus, silicon or a trace metal often becomes the limiting factor for phytoplankton growth. Since phytoplankton need these elements in appropriate ratios to build specific molecules, one element usually becomes depleted before all others and impedes growth and reproduction.

5.3.1 Population growth and nutrient limitation

In regions of the ocean with strong seasonal variations, blooms of phytoplankton occur in the spring and summer, as observed in the Norwegian Sea and illustrated in Fig. 5.4a,b: a rapid increase in phytoplankton abundance, indicated by the concentration of chlorophyll *a*, a pigment which all phytoplankton produce to harvest light, is accompanied by the consumption of nitrate and other nutrients within the euphotic layer. In this case, nitrate is completely depleted at the height of the bloom and growth is halted. Consumption of the phytoplankton by predators continues, so the abundance of chlorophyll subsequently declines rapidly.

Blooms arrested by nutrient limitation are also seen in laboratory populations. Consider a vessel of nutrient-enriched, sterilised seawater seeded with a living culture of phytoplankton cells illustrated in Fig. 5.5: during the early stages of growth, there is an exponential increase in population density, X (cells ml^{-1}), such that $X(t) \sim X(0)e^{\mu t}$ and cells divide roughly once a day (Fig. 5.5a); here μ is a population growth rate (s^{-1}) and t is time (s). Nitrate is consumed rapidly during the growth phase and the C:N ratio of the cells decreases as plentiful nitrate is rapidly imported. After three days, nitrate is completely depleted (Fig. 5.5b), rapid growth is halted and the C:N ratio of the cells increases (Fig. 5.5c). In contrast to the bloom observed in the ocean (Fig. 5.4), the laboratory population does not immediately decline when nitrate is depleted, but persists. This difference in response reflects the lack of predators in the laboratory study, where the loss of living phytoplankton cells is much reduced.

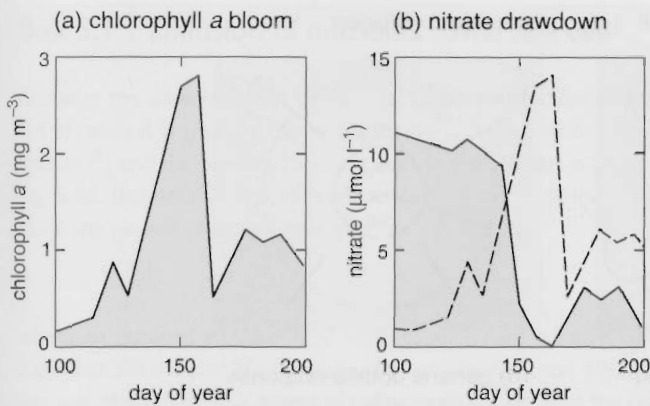


Figure 5.4 An observed phytoplankton bloom: (a) bloom of surface chlorophyll a (mg m^{-3}), and (b) drawdown of surface nitrate ($\mu\text{mol l}^{-1}$ full line, and chlorophyll repeated as dashed line) at Ocean Weather Station M in the Norwegian Sea (66°N , 2°E) in 1992. Redrawn from Dale *et al.* (1999); data provided by Francisco Rey.

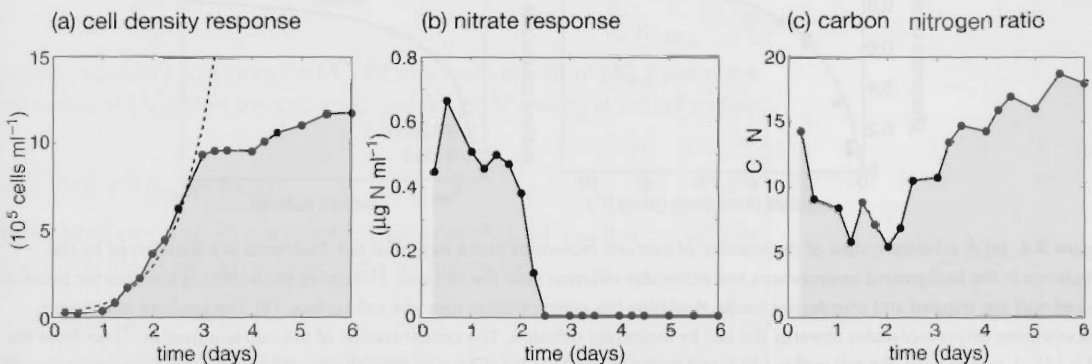


Figure 5.5 The rate of change of (a) cell number density (X , $10^5 \text{ cells ml}^{-1}$), (b) nitrate concentration ($\mu\text{g N ml}^{-1}$) and (c) carbon : nitrogen ratio in the cells from a laboratory batch culture of the marine diatom *Thalassiosira pseudonana*. A seed population was introduced into a nutrient-rich, well-lit medium. The phytoplankton population increased exponentially, consuming nitrate and other nutrients. Eventually nitrate was depleted to a limiting concentration and the population ceased to grow. The initial growth phase can be described by an exponential increase and the laboratory data in (a) are overlain by a dashed curve with an exponential growth rate $\mu = 0.75 \text{ day}^{-1}$. Note that the carbon to nitrogen ratio of these particular cells is typically greater than the Redfield ratio and varies over the course of the experiment, acquiring extra nitrogen for pigments or protein production when it is plentiful. (Data provided by Keith Davidson; Davidson *et al.*, 1999.)

Next we consider in more detail how phytoplankton and other microbes bring dissolved nutrients into the cell, and how the uptake rate is related to the nutrient concentration in the environment.

5.3.2 How do microbes acquire dissolved nutrients from the water?

The uptake of dissolved nutrients by microbial cells can be viewed in terms of two stages, as depicted schematically in Fig. 5.6a: molecules of nutrient near the cell surface are captured by transporter proteins in the cell wall and then transferred into the interior of the cell. This

uptake creates a gradient in the nutrient concentration within a narrow layer of fluid adjacent to the cell wall, which leads to a transfer of more nutrient molecules towards the cell by molecular diffusion (Fig. 5.6b).

Laboratory cultures reveal that cellular uptake of dissolved nutrients varies with the ambient nutrient concentration in the environment following a saturating function (Fig. 5.6c): when the nutrient is scarce, uptake is linearly dependent on its concentration, and when the nutrient is abundant, uptake saturates to a maximum value.

We now consider nutrient transport into and towards the cell in more detail.

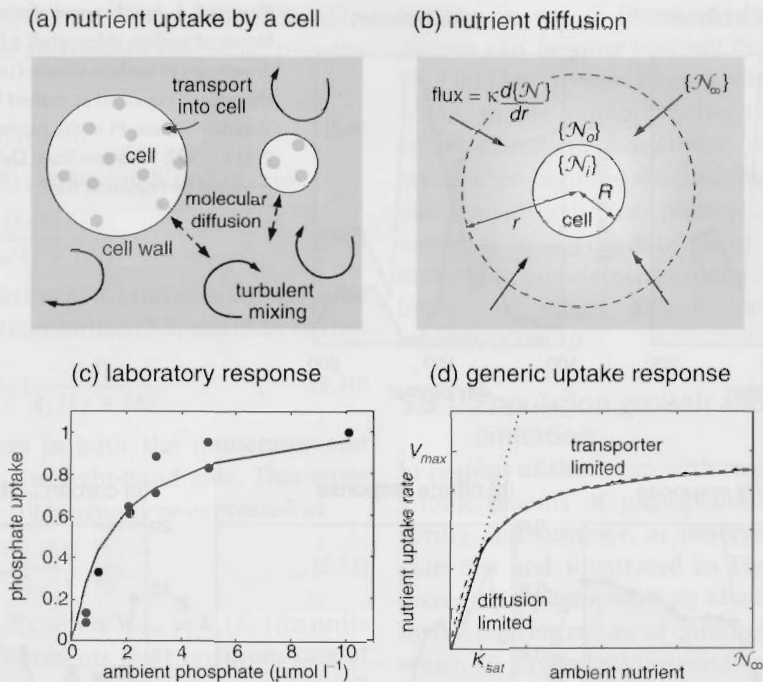
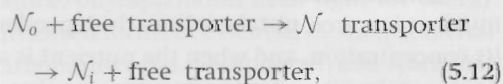


Figure 5.6 (a) A schematic view of the transfer of nutrient molecules into a microbial cell. Nutrients are transferred by the turbulence in the background environment and molecular diffusion near the cell wall. Molecules encountering transporter proteins at the cell wall are trapped and transferred inside, depleting the concentration near the cell surface. (b) The gradient in nutrient concentration drives molecules towards the cell by molecular diffusion. The concentration of the nutrient (mol m^{-3}) far from the cell is $\{N_\infty\}$, just outside the cell wall is $\{N_0\}$, and inside the cell is $\{N_i\}$. Close to the cell, the diffusive flux of N towards the cell is $\kappa d\{N\}/dr$ where κ is the molecular diffusivity and r is the radius from the centre of the cell. (c) Observed relationship between the cellular uptake of phosphate ($\text{pmol P cell}^{-1} \text{h}^{-1}$) and its ambient concentration in a laboratory culture of phytoplankton. A Michaelis–Menten curve is superimposed, with maximum uptake rate $V_{\max} = 1.1 \text{ pmol P cell}^{-1} \text{h}^{-1}$ and half-saturation coefficient $K_{\text{sat}} = 1.5 \mu\text{mol PO}_4^- \text{l}^{-1}$. Redrawn from Yamamoto and Tarutani (1999). © Wiley. (d) Cellular nutrient uptake ($\text{mol cell}^{-1} \text{s}^{-1}$) as a function of the ambient nutrient concentration in the surrounding medium. At high concentrations uptake is limited by the density and efficiency of transporters in the cell wall (dashed line). At low concentrations uptake is limited by the rate of diffusion towards the cell (dotted line). The combined result (solid black line, lesser of the dashed and dotted curves) reflects the form of the Michaelis–Menten curve, which is often fitted empirically.

Nutrient transfer across the cell wall

Transporter proteins in the cell wall capture nutrient molecules and pass them into the cell, as depicted simply in Fig. 5.6a: each transporter site is either unoccupied and ready to accept a nutrient molecule or is already engaged in the process of transport through the cell wall. Schematically, the uptake of a nutrient resource N can be represented as a two-stage process,



where N_0 is a nutrient molecule just outside the cell, $N \text{ transporter}$ represents a transporter occu-

pled by a nutrient molecule and N_i is the nutrient molecule in the cell. This two-stage nutrient uptake in (5.12) is analogous to the enzymatic reaction (5.4); also see Q5.2. Following the steps in Section 5.2.2, an analogy of the Michaelis–Menten relationship emerges between the cellular rate of uptake and the near-surface, external nutrient concentration, $\{N_0\}$:

$$\text{uptake of } N = V_{\max} \frac{\{N_0\}}{K_{\text{sat}} + \{N_0\}} \quad (5.13)$$

Here, the maximum uptake rate, $V_{\max} = E_T K_p$, depends on the density of transporters in the cell wall, E_T and the rate at which captured ions are transferred into the cell, K_p . However, this

Box 5.1 | Diffusion of nutrients towards a cell

Consider the down-gradient diffusion of nutrient molecules towards a spherical cell of radius R (m) where the ambient nutrient concentration in the fluid is $\{N_\infty\}$ (mol m^{-3}) and the concentration just outside the cell wall is $\{N_0\}$, as depicted in Fig. 5.6b. The diffusive flux of nutrients ($\text{mol m}^{-2} \text{ s}^{-1}$) towards the cell along a radial line normal to its surface is given by

$$\kappa \frac{d\{N\}}{dr},$$

where an outward increase in N leads to an inward diffusive flux and κ is the molecular diffusivity of N in seawater ($\text{m}^2 \text{ s}^{-1}$) (see Section 3.2.3). Integrating the flux over the surface of a sphere of radius much greater than the cell, $r > R$, then the area-integrated flux of N towards the cell (mol s^{-1}) is

$$4\pi r^2 \kappa \frac{\partial\{N\}}{\partial r}. \quad (5.14)$$

Applying boundary conditions for $\{N\}$ far away from the cell of $\{N_\infty\}$ and at the cell surface of $\{N_0\}$, then the area-integrated flux of N arriving at the cell surface is

$$4\pi R \kappa (\{N_\infty\} - \{N_0\}). \quad (5.15)$$

At the same time, the volume of the cell varies as $(4/3)\pi R^3$, so that the diffusive supply of nutrients per unit volume of the cell is given by

$$3\kappa (\{N_\infty\} - \{N_0\})/R^2. \quad (5.16)$$

Hence, the diffusive supply is more efficient in sustaining the growth and division of cells with a small radius R than a large radius.

relationship is couched in terms of the nutrient concentration just outside the cell wall, $\{N_0\}$, rather than the ambient concentration in the medium, $\{N_\infty\}$, which is measured in the field or laboratory, as in Fig. 5.6b. How are the near-surface nutrient concentration, $\{N_0\}$, and ambient concentration, $\{N_\infty\}$, related?

Molecular diffusion toward the cell

We assume that nutrients diffuse across a thin molecular boundary layer surrounding a spherical cell (Pasciak and Gavis, 1974; Armstrong, 2008), although fine-scale turbulence, sinking or swimming can also be important for larger cells. The cellular uptake of N is sustained by the diffusive flux into the cell surface, which (as described in Box 5.1 also see Q5.3) can be represented as

$$\text{uptake of } N = 4\pi R \kappa (\{N_\infty\} - \{N_0\}), \quad (5.17)$$

where R is the radius of the cell.

The two views of nutrient uptake described by (5.13) and (5.17) must, in reality, be consistent and the near-cell concentration, $\{N_0\}$, will adjust to reflect this. The two expressions can be combined to eliminate N_0 , solving for uptake in terms of N_∞ , transporter density and molecular diffusion characteristics (see Armstrong, 2008). Here, more simply, we consider two limits:

- If diffusion towards the cell is the rate-limiting process, then the near-cell concentration will become strongly depleted so $\{N_\infty\} \gg \{N_0\}$ and, from (5.17), the uptake rate is given by

$$4\pi R \kappa \{N_\infty\}. \quad (5.18)$$

This limit is most likely to occur at low ambient nutrient concentrations. Uptake is linearly dependent on the ambient concentration of the nutrient and is not limited by the density of transporters (represented by V_{max}).

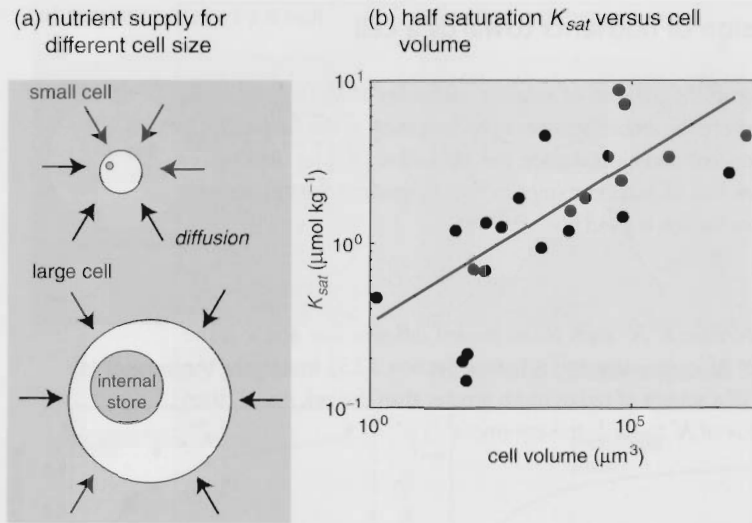


Figure 5.7 The effect of cell size on nutrient uptake and storage. (a) Schematic view: nutrients used for growth are supplied either externally by diffusion into the cell (arrows) or from an internal store of previously acquired nutrient. Diffusion is more efficient for smaller cells. Larger cells can accommodate a larger, easily accessible internal store of nutrients. (b) The half-saturation coefficient, K_{sat} ($\mu\text{mol kg}^{-1}$), for the nitrate uptake rate ($\text{mol N cell}^{-1} \text{s}^{-1}$) by phytoplankton as a function of cell volume, based on a compilation of laboratory culture studies. Smaller cells have lower half saturations and are more effective at directly obtaining nutrients from the environment. Redrawn from Litchman et al. (2007).

- At high ambient nutrient concentrations, the diffusive flux towards the cell can supply more nutrient than the cell wall transporters can process, which reduces the deficit in the near-cell nutrient concentration, and decreases the gradient of \mathcal{N} across the boundary layer until $\{\mathcal{N}_\infty\} \sim \{\mathcal{N}_0\}$. In this limit (5.13) can be rewritten in terms of the ambient nutrient concentration

$$\text{uptake of } \mathcal{N} = V_{max} \frac{\{\mathcal{N}_\infty\}}{K_{sat} + \{\mathcal{N}_\infty\}} \quad (5.19)$$

In this case, uptake of nutrients is proportional to V_{max} and so depends on the density of transporters and the rate at which captured ions are transferred into the cell. Cells may acclimate, adjusting the density of transporters according to the ambient nutrient concentration.

Hence, these limit cases suggests that cellular nutrient uptake is either limited at low ambient nutrient concentrations by diffusion towards the cell (5.18) or at high nutrient concentrations by the density of the transporters in the cell wall (5.19). This combined response is illustrated in Fig. 5.6d and is consistent with the form of the illustrated laboratory study (Fig. 5.6c). The math-

ematical similarity with enzyme kinetics arises, in part, because both can be described as a multi-stage process characterised by an 'arrival stage' and a 'handling stage'. In this case, the arrival of nutrients at the transporter sites is modulated by the diffusive boundary layer, which is ultimately affected by larger-scale turbulence.

5.3.3 Nutrient uptake and population growth

There is an enormous diversity of phytoplankton cells. Cell size is one important factor which affects the uptake of nutrients and growth rates. Now we consider how nutrient uptake varies with size and then how nutrient uptake and growth are related.

Nutrient uptake and cell size

Cell size affects the diffusive supply of nutrients, as depicted in Fig. 5.7a: for an idealised, spherical cell at low nutrient concentrations, the diffusive supply of nutrients increases with cell radius R (5.18), but at the same time the cell volume increases as $(4/3)\pi R^3$. Thus, the diffusive supply of nutrients per unit volume is largest for cells with small R and smallest for cells with large R , see

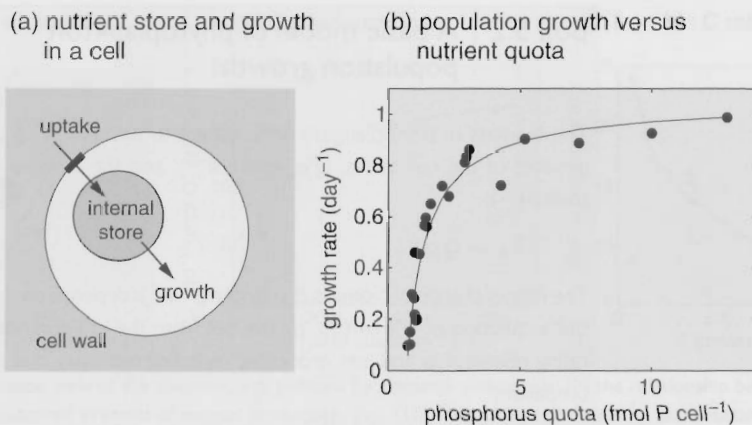


Figure 5.8 Reproduction of phytoplankton cells depends on the internal store of nutrients within the cell, as well as the uptake of nutrients from the environment. (a) A schematic view: nutrients are taken up across a cell wall into an internal store. This rapidly accessible reservoir within the cell can sustain rapid growth even when the direct uptake is insufficient at the time. (b) A laboratory view of the population growth rate, μ (day^{-1}), in continuous cultures of the phytoplankton *Monochrysis lutheri* as a function of the average phosphorus content of the cells (data from Burmaster, 1979); the solid curve is described by $\mu = \mu^{\max} \frac{\Delta Q_P}{\Delta Q_P + K_{Q_P}}$, where $\mu^{\max} = 1.05 \text{ day}^{-1}$, $K_{Q_P} = 0.75 \text{ fmol P cell}^{-1}$, $\Delta Q_P = Q_P - Q_P^{\min}$ and $Q_P^{\min} = 0.702 \text{ fmol P cell}^{-1}$; note $\text{fmol} = 10^{-15}$ moles. Larger phosphorus content implies a larger internal store, facilitating rapid growth. It may also be associated with a high concentration of RNA, which synthesises new proteins.

Box 5.1 and Q5.3. In accord with this view, laboratory studies reveal the nitrate uptake half saturation is smaller for smaller volume cells, illustrated in Fig. 5.7b, enhancing their ability to compete for nutrients at low concentrations.

Hence, if phytoplankton growth only depended on the diffusive supply of nutrients, then the fastest growing and most competitive phytoplankton species would always be the smallest cells. However, this is not the case and large cells dominate some environments.

Decoupling of nutrient uptake and growth

The uptake of nutrients and growth of new cells need not always be tightly coupled. Instead cells may acquire nutrients into an internal store then synthesise new proteins later (Fig. 5.8a). This process is analogous to a piper playing the bagpipes: the piper blows into the instrument, supplying air which does not immediately make a note, but is stored in a reservoir and used to produce notes at a later time.

Larger phytoplankton cells can accommodate an internal store of nutrients within their greater volume. When there are appropriate conditions for growth, such as sufficient sunlight, larger phytoplankton cells can utilise this store to

grow much faster than smaller cells, which are constrained by the external diffusive supply of nutrients. Laboratory studies reveal growth rate increasing with the phosphorus content of the cells, referred to as cell quota, as illustrated in Fig. 5.8b. There is a minimum cell quota, Q_P (mol cell^{-1}), necessary for survival and then cell division rate increases with cell quota, saturating at an upper bound.

Hence, growth rate increases when the cell has an internal store of phosphorus which may be accessed rapidly (Droop, 1968; Caperon, 1968). This decoupling of uptake and growth provides a mechanism by which large cells, in some circumstances, can be more viable and outcompete smaller cells. This mechanism can be described in relatively simple model structures, as in Box 5.2.

Now we consider other environmental factors affecting phytoplankton growth, and their distribution in the ocean.

5.3.4 How does light affect microbial growth?

Phytoplankton obtain energy by absorbing photons with light-harvesting pigments, as illustrated in Fig. 5.9a. Light-harvesting pigments are occupied for a finite time as the energy is passed into

Box 5.2 A basic model of phytoplankton population growth

The biomass of phytoplankton with respect to element \mathcal{N} , $B_{\mathcal{N}}$ (mol m^{-3}), is the product of the cell quota, $Q_{\mathcal{N}}$ (mol cell^{-1}), and the number density of cells, X (cells m^{-3}):

$$B_{\mathcal{N}} = Q_{\mathcal{N}}X. \quad (5.20)$$

The rate of change of biomass, $B_{\mathcal{N}}$ ($\text{mol m}^{-3} \text{ s}^{-1}$), depends on the balance between the acquisition of nutrient \mathcal{N} by the cell from the environment following a saturating relationship and loss processes, including mortality due to viral infection or predation,

$$\frac{dB_{\mathcal{N}}}{dt} = V_{\mathcal{N}}^{\max} \frac{\{N\}}{\{N\} + K_{\mathcal{N}}} X - mB_{\mathcal{N}}, \quad (5.21)$$

where $\{N\}$ is the nutrient concentration (mol m^{-3}) in the environment, $K_{\mathcal{N}}$ is the half-saturation rate (mol m^{-3}), $V_{\mathcal{N}}^{\max}$ is the cellular uptake rate ($\text{mol cell}^{-1} \text{ s}^{-1}$) and the loss of biomass is represented by a simple, linear decay, with constant m (s^{-1}).

The rate of change of number density of cells, X , is described as the balance between production due to cell division, with exponential growth rate, μ (s^{-1}), and losses due to mortality, m ,

$$\frac{dX}{dt} = \mu X - mX. \quad (5.22)$$

This simplified framework is completed by relating the growth rate, μ , to the cell quota, $Q_{\mathcal{N}}$, assuming a saturating relationship (Fig. 5.8b) following Caperon (1968),

$$\mu = \mu^{\max}(T, I) \frac{\Delta Q_{\mathcal{N}}}{\Delta Q_{\mathcal{N}} + K_{Q_{\mathcal{N}}}}, \quad (5.23)$$

where $\mu^{\max}(T, I)$ is the maximum growth rate and $\Delta Q_{\mathcal{N}} = Q_{\mathcal{N}} - Q_{\mathcal{N}}^{\min}$ is the excess of nutrient element \mathcal{N} relative to its minimum subsistence quantity, and $K_{Q_{\mathcal{N}}}$ is a half-saturation coefficient. The maximum growth rate may be modulated by other environmental variables, including temperature (T) and light (I).

the cell before being able to absorb additional photons; see Falkowski and Raven (1997) for a detailed exposition on aquatic photosynthesis. Primary production, the creation of organic matter, generally increases with the incident flux of photons at low light levels, but saturates at high photon fluxes, as illustrated in Fig. 5.9b. Conceptually the form of this relationship is analogous to an enzymatic reaction with an arrival stage and a handling stage.

Phytoplankton adjust the abundance of pigment in the cell, the chlorophyll concentration, to optimise light harvesting. In reduced irradi-

ence, the cells produce a higher concentration of chlorophyll (Fig. 5.9c), reflected in the increasing chlorophyll content of phytoplankton with depth through the euphotic zone, as observed in the tropical Atlantic in Fig. 5.10, even though carbon biomass remains uniform over the same layer. This acclimation of chlorophyll in phytoplankton alters the elemental composition of the cells, since pigments used for light harvesting are rich in nitrogen (Geider *et al.*, 1997).

Conversely, if irradiance is very strong, the cellular chlorophyll concentration is reduced. Under some circumstances, the increased incidence of

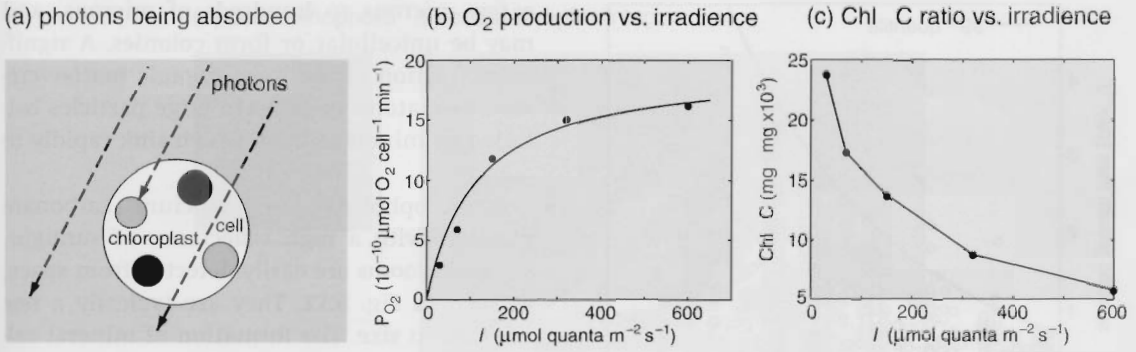


Figure 5.9 (a) A schematic view of the absorption of photons by pigments within cells; (b) the relationship between gross photosynthesis measured in terms of oxygen production, P_{O_2} ($10^{-10} \mu\text{mol O}_2 \text{ cell}^{-1} \text{ min}^{-1}$), and irradiance, I ($\mu\text{mol quanta m}^{-2} \text{ s}^{-1}$) by visible wavelength radiation in equilibrated laboratory cultures of *Isochrysis galbana*; and (c) the acclimated ratio of cell chlorophyll to carbon content, Chl : C ($\text{mg : mg} \times 10^3$), in the same cultures. At low light, the cells increase chlorophyll content in an effort to maintain light-harvesting capability. Data from Falkowski *et al.* (1985).

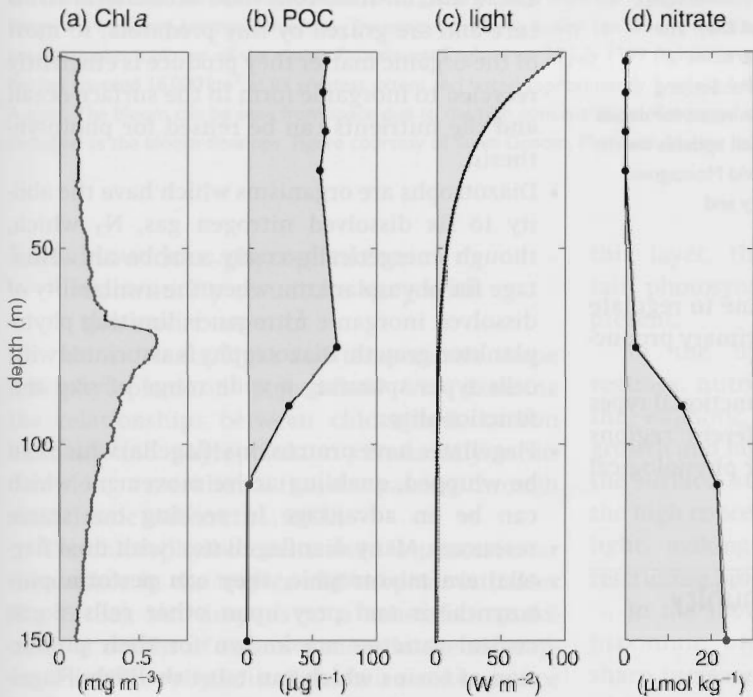


Figure 5.10 Vertical profiles of (a) chlorophyll *a* (mg m^{-3}) and (b) particulate organic carbon, POC ($\mu\text{g l}^{-1}$), including total phytoplankton and zooplankton biomass, (c) the downward flux of visible wavelength solar radiation (W m^{-2}) and, (d) nitrate concentration ($\mu\text{mol kg}^{-1}$) in the equatorial Atlantic Ocean (2.5°N , 24.4°W). Data from Atlantic Meridional Transect 15; figure courtesy of Anna Hickman.

photons is damaging and photosynthesis becomes less efficient as light exposure increases. In this case, resources within the cell are diverted to form photo-protection pigments, which dissipates the excess energy and protects the cell, at the price of a reduced rate of photosynthesis and population growth.

5.3.5 How does temperature affect phytoplankton growth?

Biochemical reactions proceed more rapidly at warmer temperatures; accordingly laboratory studies reveal maximum phytoplankton growth rates increase with temperature (Fig. 5.11). In the ocean, the effects of nutrient availability,

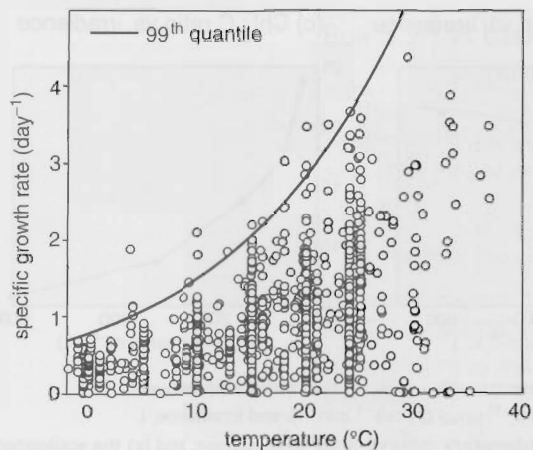


Figure 5.11 Marine phytoplankton, maximum growth rate (day^{-1}) as a function of temperature (circles), each point represents the measured growth rate of a phytoplankton culture at a particular temperature from a dataset of 1501 samples, together with the 99th regression quantile (full line). The envelope of highest maximum growth rates increases exponentially with temperature, reflecting the underlying temperature sensitivity of biochemical reaction rates; for details of the data set, see Bissinger *et al.* (2008), which updates the study of Eppley (1972). Figure courtesy of David Montagnes, © 2008 by the American Society of Limnology and Oceanography.

irradiance and temperature combine to regulate phytoplankton growth rates and primary production of organic matter.

Next we consider how diverse functional types of phytoplankton flourish in different regions of the ocean, examining how their physiological adaptations make them successful.

5.4 Phytoplankton community structure

There is a vast diversity in phytoplankton species in the oceans with cell sizes ranging from one to hundreds of microns and a wide variety of physiological specialities:

- Diatoms can form large internal stores, grow very quickly and bloom when resources are plentiful. They create silicon-based structural parts, spanning a wide range of cell size from

a few microns to hundreds of microns, and may be unicellular or form colonies. A significant fraction of the fresh organic matter created by diatoms ends up in large particles ballasted by mineral silicon which sink rapidly to depth.

- Coccolithophorids form calcium carbonate platelets with a high reflectance of sunlight, so their blooms are easily detected from space, as seen in Fig. 5.12. They are typically a few microns in size. The formation of mineral calcium carbonate has a significant effect on surface ocean chemistry and provides ballast to particles, enhancing the sinking flux of organic matter.
- Tiny pico-phytoplankton dominate the ecosystem over large regions of the surface ocean. These micron-scale cells have no mineral structure and are grazed by tiny predators, so most of the organic matter they produce is efficiently recycled to inorganic form in the surface ocean and the nutrients can be reused for photosynthesis.
- Diazotrophs are organisms which have the ability to fix dissolved nitrogen gas, N_2 which, though energetically costly, can be an advantage for phytoplankton when the availability of dissolved inorganic nitrogen is limiting phytoplankton growth. Diazotrophy is associated with cells types spanning a wide range of size and functionality.
- Flagellates have protrusions (flagella) which can be whipped, enabling active movement which can be an advantage in seeking out scarce resources. Many dinoflagellates (with dual flagella) are mixotrophic; they can perform photosynthesis and prey upon other cells. Some coastal varieties are known for their production of toxins which can taint shellfish. Flagellates range from a few microns to hundreds of microns in size.

Each of these key phytoplankton groups is composed of many hundreds or thousands of species and physiological variants. Next we consider in more detail the relationships between light, nutrients, phytoplankton abundance and community structure.

(a) coccolithophore (b) coccolithophore bloom

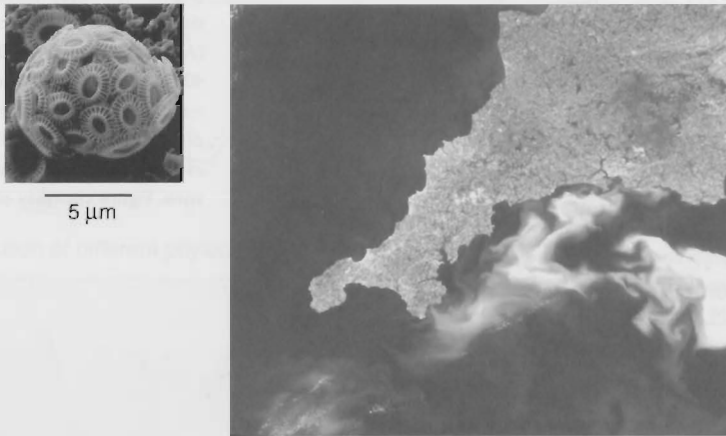


Figure 5.12 (a) Electron-micrograph of coccolithophores; unicellular marine phytoplankton which form calcium carbonate platelets, perhaps as protection from grazers. Image from Karl-Heinz Baumann Universität Bremen (<http://www.geo.uni-bremen.de/cocco>). The species *Emiliania huxleyi* can bloom, reaching high concentrations, (b) Landsat image of a coccolithophore bloom off the coast of southwest England on 24 July 1999 (lighter is more reflectance). The high-reflectance patch (white) covered 16 000 km² at its greatest extent and lasted approximately 3 weeks before being dispersed by unsettled weather in August. The bloom can be seen from space due to the high concentration of external calcite platelets or coccoliths that become detached as the bloom develops. Figure courtesy of Steve Groom, Plymouth Marine Laboratory; see Smyth *et al.* (2002).

5.4.1 How does phytoplankton community structure vary with the environment?

How do nutrients, light and temperature shape the phytoplankton population? We examine the relationships between chlorophyll, carbon biomass, and phytoplankton community structure along a meridional transect passing through the Atlantic (Aiken *et al.*, 2000).

The chlorophyll concentration is greatest near the surface in the tropics and subpolar latitudes (Fig. 5.13a), but deepens to a subsurface maximum at depths of 100 m or more in the subtropics. This chlorophyll distribution is a consequence of both light and nutrient availability. The depth at which the downward flux of solar radiation is reduced to 1% of its surface value is often used as a measure of the euphotic layer depth, and varies from a few metres, where phytoplankton pigments or suspended sediments are abundant, to as much as 200 m in the clearest waters of the open ocean, where most of the photons are absorbed by water molecules (Fig. 5.13, dashed line). Below

this layer, there is insufficient light to sustain photosynthesis and few phytoplankton are present.

In the upwelling tropical and subpolar regimes, nutrient-rich waters are delivered into the euphotic zone, sustaining phytoplankton growth and high chlorophyll concentrations near the surface, at least on a seasonal basis. In turn, the high concentration of surface pigment absorb light, making the euphotic layer thinner and restricting production at depth.

In the subtropics, the subsurface chlorophyll maximum broadly follows the nitracline, the sharp increase in nitrate with depth (Fig. 5.13b), which is also coincident with the base of the euphotic zone (Fig. 5.13, dashed line), suggesting close co-regulation of phytoplankton growth by nutrient and light availability.

How does phytoplankton community structure vary?

Along a similar meridional section, the near-surface carbon biomass closely follows the

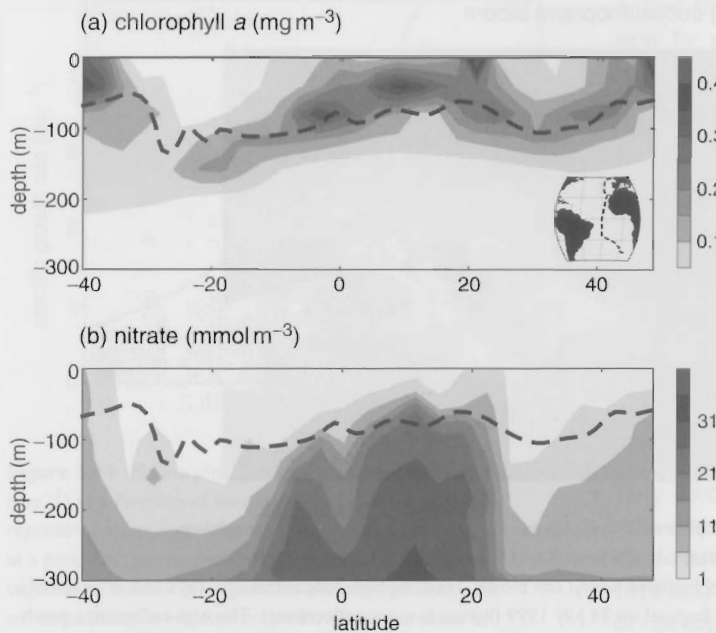


Figure 5.13 Observed (a) chlorophyll *a* (mg m^{-3}), and (b) nitrate (mmol m^{-3}) with depth along the Atlantic Meridional Transect (AMT15, September 2004) from 50° N to 40° S in the Atlantic Ocean. Dashed contours indicate the depth at which irradiance is 1% of the incident surface flux, sometimes used as an indicator of the depth of the euphotic zone. Figure courtesy of Anna Hickman.

near-surface chlorophyll *a* distribution (Fig. 5.14a), which reflects the contribution of different phytoplankton species (Fig. 5.14b):

- Diatoms occur in the nutrient-rich, surface waters of the tropics, subpolar latitudes and off coastal upwelling sites.
- Pico-cyanobacteria, including *Prochlorococcus* and *Synechococcus*, as well as flagellates dominate in the nutrient-depleted regions of the subtropics.
- Coccolithophorids are ubiquitous, but typically account for only 2 to 10% of total phytoplankton biomass along this transect (Marañón *et al.*, 2000).
- Nitrogen-fixing phytoplankton have been observed over the tropics and subtropics, extending up to latitudes of typically 30° though they make a very minor contribution to biomass.

Now we consider in more detail why the phytoplankton community structure varies with the environment in this way along the Atlantic Meridional Transect, and as illustrated in a global ecosystem model in Plate 16.

5.4.2 What regulates the pattern of community structure?

The biogeography of the marine ecosystem, what lives where and when, is determined by the relative fitness of all of the possible organism physiologies in different environments. We can make a broad brush interpretation by classifying many phytoplankton into one of two types: “gleaners” adapted to low nutrient conditions, and “opportunists” which can most efficiently exploit resources when they become plentiful (MacArthur and Wilson, 1967).

Gleaners and low nutrient conditions

Gleaners specialise in efficiently acquiring resources when they are sparse. Near-surface waters over the subtropical oceans are depleted in dissolved inorganic nutrients, as illustrated in Fig. 5.13b, while irradiance remains strong in these clear waters. The smallest phytoplankton, the cyanobacterium *Prochlorococcus*, dominate this stable environment (Fig. 5.14). Their small size makes them efficient gleaners, with low half-saturation coefficients and efficient diffusive uptake of nutrients (Box 5.3). Flagellates are also

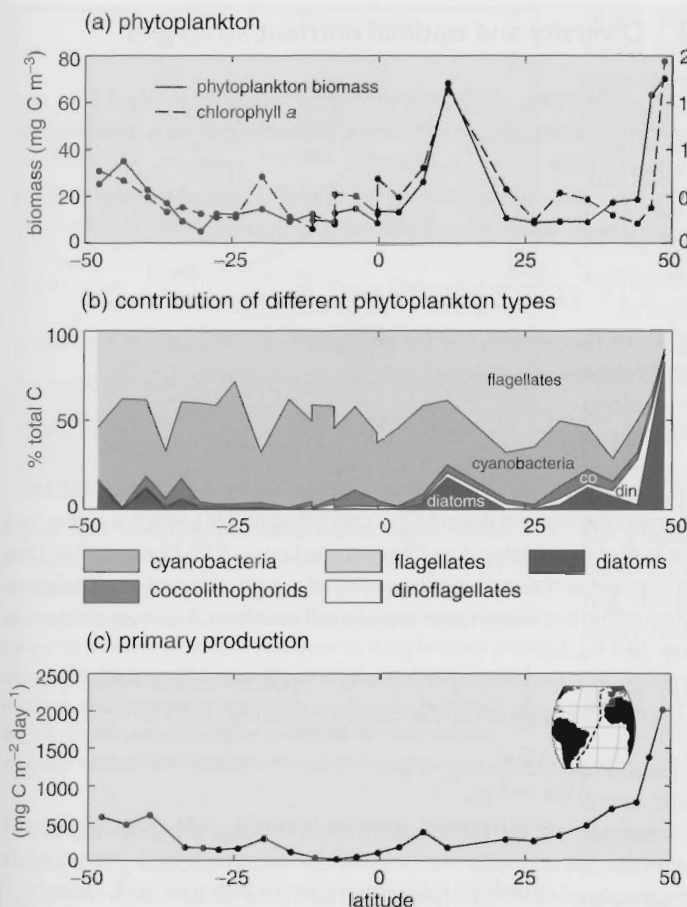


Figure 5.14 Observed phytoplankton community characteristics at 7 m depth along the Atlantic Meridional Transect (AMT2, May 1996): (a) phytoplankton biomass (mg C m^{-3} full line) and chlorophyll *a* concentration (mg m^{-3}); (b) contributions to biomass of functional groups (mg C m^{-3}), cyanobacteria (mid grey), coccolithophorids (dark grey), flagellates (light grey) and dinoflagellates (white), and diatoms (very dark grey); (c) primary production ($\text{mg C m}^{-2} \text{ day}^{-1}$). Redrawn from Marañón *et al.* (2000), with help from X. Irigoien.

abundant in the subtropics. Their flagella provide a means to move and escape a locally depleted nutrient environment at scales close to their own size.

Opportunists and high nutrient conditions

In contrast, opportunists are organisms which can grow rapidly when resources are plentiful. The mid- and high-latitude oceans are strongly seasonal: winter mixing supplies nutrients to the surface and in the following spring, when the water column warms and irradiance increases, there is a window of opportunity when all resources are replete. These optimal conditions fuel a bloom of opportunists, typically fast-growing diatoms, as illustrated in Fig. 5.4. On shorter timescales, the surface ocean is also regularly disturbed by

the passage of weather systems and ocean eddies, which can enable opportunistic phytoplankton to thrive intermittently.

Alternative strategies

There are also other ecologically successful strategies. For example, mixotrophic dinoflagellates combine photosynthesis with an ability to prey upon other cells; they are successful in environments where neither fast-growing opportunists nor more efficient gleaners survive, and can thrive in barren periods by eating their competitors (Thingstad *et al.*, 1996). Nitrogen fixers also flourish in nitrate-depleted, subtropical waters, where they relieve nitrogen limitation by expending energy to break the triple bond in nitrogen gas at the price of reduced growth rate.

Box 5.3 | Diversity and optimal nutrient strategies

Consider the simple model of phytoplankton growth outlined in Box 5.2 for two contrasting regimes, an equilibrium state where seasonal variability is relatively small and a time-varying state.

Consider the equilibrium solution for the rate of change of biomass (5.21) in a tightly coupled state, where growth and mortality balance.

$$\frac{dB_N}{dt} = V_N^{\max} \frac{\{N\}}{\{N\} + K_N} X - mQ_N X \sim 0, \quad (5.24)$$

which can be rearranged to define the equilibrium concentration of the limiting nutrient, $\{N\}$, in terms of the physiology of the phytoplankton community,

$$\{N\} = \frac{K_N m}{V_N^{\max}/Q_N - m}. \quad (5.25)$$

In this limit, the organism which can exist at the lowest equilibrium nutrient concentration draws the nutrient down to this concentration $\{N\}$, which is below the subsistence level of their competitors (Stewart and Levin, 1973; Tilman, 1977). The equilibrium nutrient concentration is a function of the physiological characteristics of the phytoplankton and a low nutrient uptake half saturation, K_N is advantageous for a gleaner (see Fig. 5.7b).

Alternatively, in a time-varying environment, opportunists can instead thrive. Consider the rate of change of number density, combining (5.22) and (5.23):

$$\frac{dX}{dt} = \mu^{\max} \frac{\Delta Q_N}{\Delta Q_N + K_{Q_N}} X - mX. \quad (5.26)$$

In a variable environment, the fittest opportunist is the organism which capitalises most effectively on the availability of an intermittent resource, boosting their population during the plentiful periods in preparation for the barren periods. From (5.26), the per capita net growth rate for a population of phytoplankton is described as

$$\frac{1}{X} \frac{dX}{dt} = \mu^{\max} \frac{\Delta Q_N}{\Delta Q_N + K_{Q_N}} - m. \quad (5.27)$$

The organism with the highest per capita growth rate is the most effective opportunist. This optimal response can be achieved in a variety of ways: to have a large maximum growth rate, μ^{\max} ; to maintain a large internal store of readily available nutrient resources, ΔQ_N ; or to reduce mortality, m , by defence against predators.

Now we turn to the integrated effect of these different phytoplankton species on the formation of organic carbon and its subsequent fate.

5.5 | Primary production and the fate of organic matter

The production of organic carbon, referred to as primary production, depends upon several fac-

tors: the abundance of chlorophyll and irradiance, the availability of essential nutrients and temperature. Primary production is separated into two components: new production utilises nutrients recently arrived into the euphotic layer, while recycled production utilises nutrients derived from respired organic matter which never left the euphotic layer (Fig. 5.15). The relative contributions of new and recycled production varies according to how much 'new' nutrients are

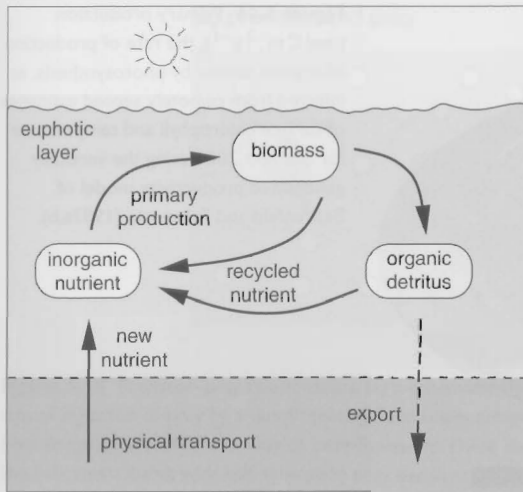


Figure 5.15 Primary production of organic matter may be fuelled in part by 'new' inorganic nutrients which have recently arrived in the local euphotic layer through physical transport or atmospheric deposition. In addition, local respiration of organic matter by bacteria or zooplankton returns living biomass and detritus to the form of inorganic nutrients, and these recycled nutrients also contribute to primary production. A fraction of organic matter, either living or in detrital form, leaves the euphotic layer; this fraction is referred to as export production.

supplied and the phytoplankton community structure.

Some of the organic matter leaves the euphotic zone and passes into the dark interior; this downwards flux of organic matter is referred to as export production. For a steady state, new production and export production have to balance each other when averaged over large space and time scales (Fig. 5.15), although this balance need not hold locally.

5.5.1 Estimating primary productivity

The rate of primary production can be evaluated using *in situ* observations, such as by measuring the rate of uptake of radiocarbon-labelled dissolved inorganic carbon or the rate of production of oxygen in a closed sample. For example, primary production measured along the Atlantic Meridional Transect in Fig. 5.14c varies from less than $300 \text{ mg C m}^{-2} \text{ day}^{-1}$ over the subtropical gyres to more than 500 and up to $2000 \text{ mg C m}^{-2} \text{ day}^{-1}$ over the subpolar latitudes.

Primary production varies strongly with the abundance of chlorophyll. More chloro-

phyll means more light energy harvested and more organic molecules produced. A productivity model using remotely sensed chlorophyll and temperature suggests that primary productivity is largest in the coastal seas, over parts of the tropics and the high latitudes, while primary productivity is lowest in the subtropical gyres and parts of the Southern Ocean (Fig. 5.16; Behrenfeld and Falkowski, 1997).

Integrated over the globe, estimates of the annual primary production range between 35 and 75 Pg C y^{-1} (Carr *et al.*, 2006). Thus, the photosynthetic production of organic matter in the euphotic layer integrated over a year is of similar order of magnitude to the total living microbial biomass in the entire global ocean (see Q5.1). Thus the global standing stock of biomass in the ocean is refreshed about once a year and the global standing stock of phytoplankton biomass is renewed every couple of weeks.

5.5.2 What is the fate of the organic matter produced by phytoplankton?

Production of organic matter by phytoplankton forms the base of the marine food chain. The subsequent fate of the organic matter is very complex (as depicted in Fig. 5.17), involving the interactions of a vast diversity of organisms and life strategies, from virus to whale. Consequently, it is very difficult to characterise and quantify the fluxes and fate of organic carbon in the marine ecosystem.

Phytoplankton ultimately die through infection by virus, consumption by predators or sinking out of the euphotic layer into the dark waters. Each of these processes leads to the formation of particulate and dissolved organic detritus, which is ultimately reworked and respired by heterotrophs, including zooplankton and bacteria.

- **Viral Infection.** A virus penetrates the cell wall and hijacks the genetic material and nutrient resources of the host cell in order to replicate. After some time the host is burst, releasing the new generation of virus and leaving the remaining portions of the cell to sink or be consumed by other organisms.
- **Predation.** The smallest, micron-scale phytoplankton, such as *Prochlorococcus*, are preyed upon by unicellular predators which can

primary production ($\text{mol C m}^{-2} \text{y}^{-1}$)

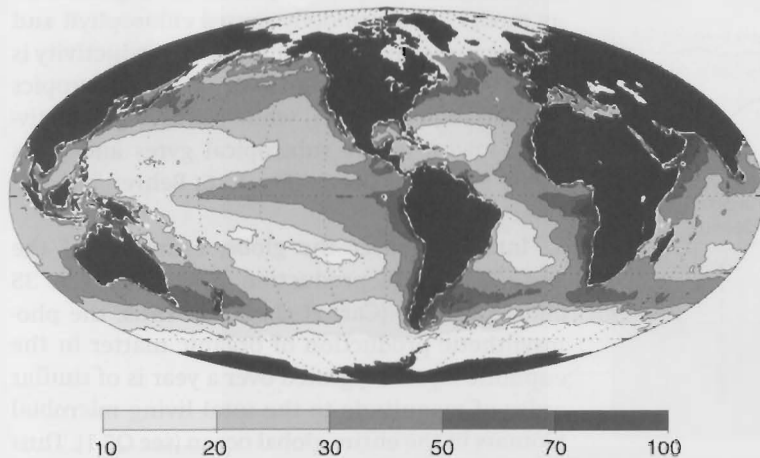


Figure 5.16 Primary production ($\text{mol C m}^{-2} \text{y}^{-1}$), the rate of production of organic matter by photosynthesis, as inferred from remotely sensed estimates of surface chlorophyll and temperature for the year 2005 using the vertically generalised productivity model of Behrenfeld and Falkowski (1997a,b).

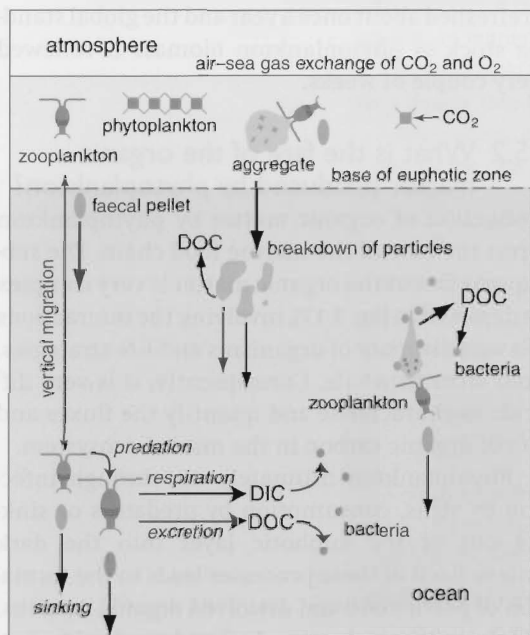


Figure 5.17 Schematic depiction of processes which regulate the export of organic matter from the euphotic layer into the deep ocean. These include primary production of organic carbon, grazing and sinking of phytoplankton cells, respiration and reworking of sinking particulates by bacteria and zooplankton. Modified from Burd *et al.* (2002).

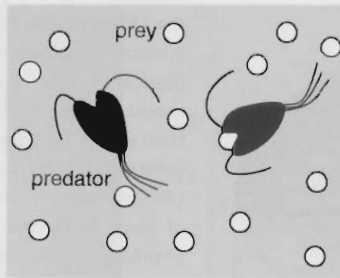
engulf whole cells and digest them. These tiny predators, or micro-zooplankton, excrete dissolved organic matter (DOM), organic detritus consisting of single molecules or tiny, neutrally buoyant particles, which in turn provide a source of nutrients and energy to bacteria.

Larger cells, including diatoms, coccolithophorids, and the micro-zooplankton are preyed upon by larger grazers, including millimetre-scale, shrimp-like copepods and jelly-like, filter-feeding salps. These predators also release DOM and sinking particulate organic matter, POM, through sloppy feeding and the production of faecal pellets.

The grazing of prey by predators can be described as a two-stage process with an interesting analogy to enzyme kinetics. Prey are captured by a predator (Fig. 5.18a), then must be ingested before another capture can occur (Holling, 1959), leading to the characteristic saturating functional form associated with arrival and handling. Laboratory studies reveal the ingestion of prey by a zooplankton increases with prey density, then saturates, as illustrated in Fig. 5.18b. This relationship can be modified by the behaviour of the predators; for example, when prey is scarce, more energy can be spent finding food than is consumed, so that a predator may stop feeding or switch to a different prey.

- **Sinking.** Small phytoplankton cells and organic matter are easily suspended by turbulence, while larger phytoplankton cells and clumps of organic matter sink more quickly. This response is analogous to how small cloud droplets in the atmosphere remain suspended until they coalesce together and form larger droplets which fall out of the cloud as rain. However,

(a) predator and prey



(b) laboratory study of grazing

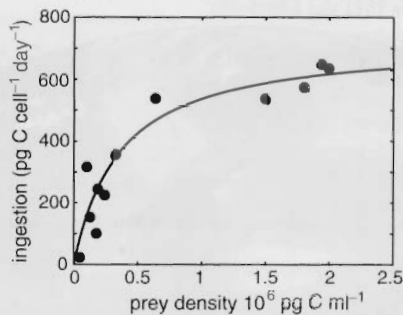


Figure 5.18 Predator–prey relationships: (a) a schematic view of a predator hunting prey, and (b) a laboratory study revealing the rate of ingestion of prey by a dinoflagellate, *Karlodinium armiger*, versus prey density of a phytoplankton, *Rhodomonas salina*; redrawn from Berge *et al.* (2008) courtesy of Inter-Research. These data can be described by a saturating curve (Holling, 1959); here the solid line indicates a curve with half-saturation prey density of $0.35 \times 10^6 \text{ pg C ml}^{-1}$ and maximum ingestion rate of $720 \text{ pg C cell}^{-1} \text{ day}^{-1}$

living cells can counteract negative buoyancy by forming a vacuole or a reservoir of low density organic compounds. In contrast, the dense mineral components of diatoms and coccolithophorids promote sinking. In the late stages of diatom blooms, the cells excrete carbon-rich organic matter which sticks together, forming sinking aggregates and marine snow (see later Fig. 5.20a). As the sinking material falls, suspended material is swept up (like falling cloud drops growing into rain drops), and provide a source of nutrition for heterotrophs living at depth.

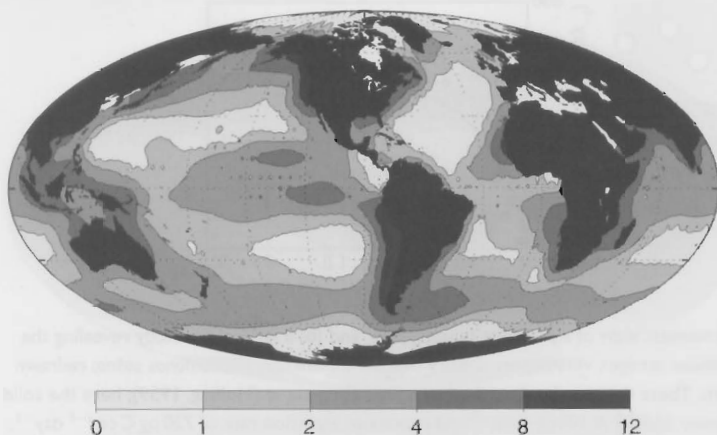
5.5.3 Export production

Most of the organic matter produced by phytoplankton is respired by bacteria or zooplankton within the sunlit euphotic layer. However, a significant fraction of organic matter is transported into the underlying dark waters. The organic matter leaves the euphotic zone either as sinking particles or suspended and transported by the circulation. The organic matter is separated into particulate organic matter (POM) and dissolved organic matter (DOM), which is operationally defined as passing through a $0.45 \mu\text{m}$ filter. DOM includes contributions from compounds consumed within hours, perhaps amino acids which can be used by other cells, to very long-lived compounds, including structural proteins, which circulate within the ocean for hundreds of years or more.

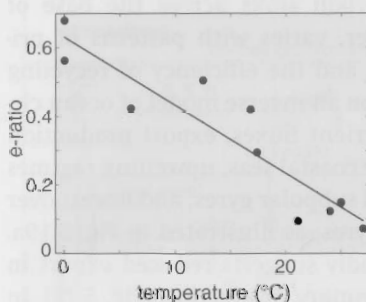
Export production, the rate at which particulate organic carbon sinks across the base of the euphotic layer, varies with patterns of primary production and the efficiency of recycling (Fig. 5.15). Based on an inverse model of ocean circulation and nutrient fluxes, export production is largest over the coastal seas, upwelling regimes in the tropics and subpolar gyres, and lowest over the subtropical gyres, as illustrated in Fig. 5.19a. This pattern broadly suggests reduced export in regions of low primary production (Fig. 5.16). In support of this view, observations with sediment traps, suspended cups which catch sinking particles, suggest that between 10% and 70% of primary production is exported from the euphotic layer as sinking particles (Fig. 5.19b,c; Laws *et al.*, 2000), with highest export efficiencies in the colder, nutrient-rich, productive waters.

Phytoplankton community composition also affects the efficiency of recycling and the resulting export production:

- Small cells without mineral parts sink more slowly and are more likely to be consumed and recycled within the euphotic layer or the upper water column. Phytoplankton with small cells preferentially flourish in the nutrient-depleted surface waters of the subtropical gyres. Hence, the ratio of export to primary production, the *e*-ratio, is low over the subtropical gyres, as illustrated in Fig. 5.19b,c.
- Larger cells, such as diatoms or coccolithophores, with mineral parts, lead to more

(a) export production ($\text{mol C m}^{-2} \text{y}^{-1}$)

(b) e-ratio versus temperature



(c) e-ratio versus latitude

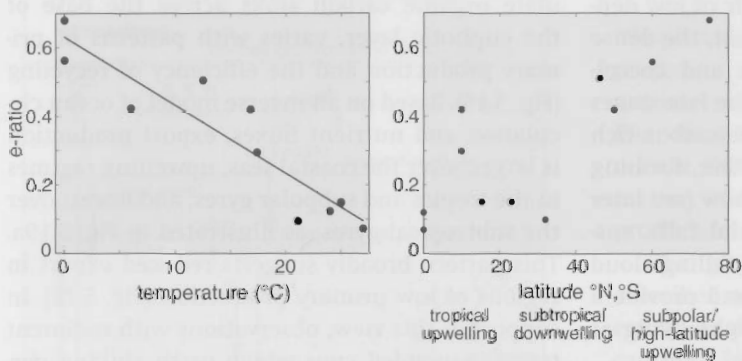


Figure 5.19 (a) Export production: the downward flux of organic carbon across the 133 m depth horizon ($\text{mol C m}^{-2} \text{y}^{-1}$) is estimated using an inverse model for the physical transport of temperature, salinity, nutrients and carbon (Schlitzer, 2000; data from export estimate provided by R. Schlitzer). In (b) and (c), the e-ratio (dimensionless) is defined as the fraction of export production (from measurements of sinking particles) divided by primary production plotted against (b) temperature ($^{\circ}\text{C}$) and (c) latitude (north or south). There is a clear relationship for the e-ratio with temperature (full line), but a more complex variation with latitude, reflecting the dynamical regime: low e-ratios in the latitude band for downwelling, subtropical gyres and larger e-ratios over the upwelling zones of the tropics, subpolar gyres and high latitudes. Data in (b) and (c) compiled by Laws *et al.* (2000) from regional process studies.

rapid sinking with their silica or calcium-carbonate mineral components deterring efficient grazing. If they are grazed, the faecal pellets of the grazers are then packed with ballast from the undigested mineral material. Larger cells tend to flourish in nutrient-rich upwelling regions, such as the tropics and subpolar waters, which then have high export relative to primary productivity, a high e-ratio (Fig. 5.19c).

Hence, the export of organic matter from the euphotic zone is affected by both the primary productivity and the phytoplankton community structure. Now we consider the subsequent fate of the organic matter.

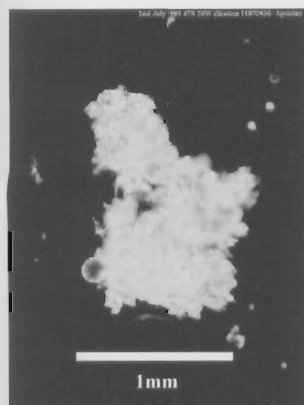
5.5.4 What is the fate of exported organic carbon?

Marine microbes have evolved to efficiently utilise the energy available from organic matter created

by primary producers. Almost all of the organic material leaving the sunlit layer is respired by heterotrophs. Immediately below the euphotic layer, the downward flux of organic matter decreases rapidly, with an e-folding length scale, z^* , of typically 100 m to 200 m (Fig. 5.20b). Only about 1% of the export from the euphotic layer reaches the sea floor, where the organic matter may be respired by benthic organisms or buried in the sediments.

Larger and denser particles sink faster and are respired at greater depth than smaller or less dense particles. A sinking speed of 100 m per day implies a particle leaves the euphotic layer within a day or two, and might take several weeks to reach the sea floor. Mineral ballast increases sinking speed and protects some of the associated organic material from bacterial respiration, leading to slower and deeper regeneration. The

(a) marine snow



(b) sinking flux of POC

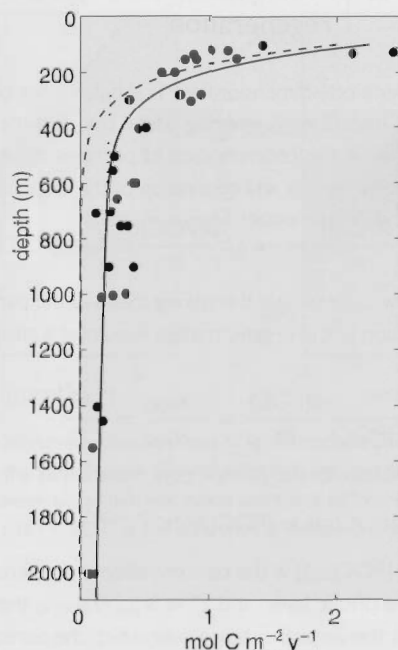


Figure 5.20 (a) Photograph of marine snow collected 2 July 1989 at 47°N, 20°W. This organic detritus, collected below the surface sunlit layer, includes aggregates of organic matter from dead organisms and faecal matter, mineral material from phytoplankton cell structures and dust particles blown from the land; courtesy of Richard Lampitt (Watson *et al.*, 2001). (b) A vertical profile of the sinking flux of particulate organic carbon in the subtropical Pacific Ocean, as measured by sediment traps; redrawn from Martin *et al.* (1987). Filled circles represent the measured data. The solid line represents the total downward flux, and dashed and dotted lines indicate modelled fluxes of unprotecte and protected particle organic carbon, respectively; the curves are $F_{\text{POC}}(z) = F_{\text{POC}}(z_0)e^{-(z-z_0)/z^*}$ where $F_{\text{POC}}(z_0)$ is 2.0 and 0.25 mol C m⁻² y⁻¹ respectively, z^* is 100 and 2500 m respectively, and the reference depth, z_0 , is 100 m (see Box 5.4).

ratio of organic carbon to calcium carbonate in sinking particles decreases from around 80% at the base of the euphotic zone to about 5% at 1000 m and deeper depths. Most of the organic carbon in the particles is readily accessible to bacteria and quickly respired, while about 5% is protected from the bacteria by the matrix of mineral material (Armstrong *et al.*, 2002); see Fig. 5.20b, dashed and dotted lines, and Box 5.4 for a mathematical representation.

Conceptually, the sinking organic particles can be separated into material protected by ballast and that which is not (Armstrong *et al.*, 2002): the two components are respired at different rates reflecting how accessible the organic matter is to bacteria. The downward flux of organic carbon can then be described as the sum of two exponentially decaying components with depth, one with a longer regeneration length scale (slower regeneration rate) than the other (curves on Fig. 5.20b). This simple model reflects some important processes, but is still highly idealised, since the rate of respiration of organic carbon depends on complex interactions with the organisms in the environment.

5.6 Consequences for ocean biogeochemistry

The recycling of exported organic matter has a major impact on the large-scale distribution and cycling of biologically active tracers in the ocean. As Redfield (1934) first noted, there is a close correspondence between the average elemental ratios in the plankton and those of the dissolved inorganic nutrients in the water column (Table 5.2).

Primary production creates organic matter with average elemental ratios of C N P = 106 : 16 : 1. This organic matter passes through the food web, some of it eventually sinking to the deep ocean to be respired by heterotrophs, returning the elements to dissolved inorganic form in approximately the same ratio. Recent inferences of the elemental ratios in sinking particles find C N P -O₂ = 117(±14) : 16(±1) : 1 : -170(±19) (Anderson and Sarmiento, 2004).

The observed relationships between dissolved inorganic carbon, nitrate and phosphate in the global ocean are thus broadly consistent with the elemental ratios of the plankton population, as

Box 5.4 A simple model of particle respiration and regeneration

Consider a one-dimensional vertical balance for organic matter in sinking particles, {POC} (mol C m^{-3}), ignoring lateral transfers. Below the euphotic layer, the rate of change in the concentration of particles depends upon the divergence of the vertical sinking flux and respiration of the organic matter,

$$\frac{\partial\{\text{POC}\}}{\partial t} = -w_{\text{sink}} \frac{\partial\{\text{POC}\}}{\partial z} - \lambda_{\text{POC}}\{\text{POC}\}, \quad (5.28)$$

where w_{sink} (m s^{-1}) is the sinking speed of the particles, and λ_{POC} (s^{-1}) the rate of respiration of the organic matter. Assuming a steady state, then rearranging (5.28) reveals

$$\frac{1}{\{\text{POC}\}} \frac{\partial\{\text{POC}\}}{\partial z} = -\frac{\lambda_{\text{POC}}}{w_{\text{sink}}} = -\frac{1}{z^*}. \quad (5.29)$$

The solution for the particle concentration as a function of depth, {POC}(z), is

$$\{\text{POC}(z)\} = \{\text{POC}(z_0)\}e^{-(z-z_0)/z^*}, \quad (5.30)$$

where {POC}(z₀) is the concentration at a reference depth, z₀, perhaps the base of the euphotic layer; and $z^* = w_{\text{sink}}/\lambda_{\text{POC}}$ is the e-folding length scale of regeneration, the vertical distance over which the particle concentration decreases by a factor e. This simple model suggests an exponential decrease in particle concentration with depth, subject to λ_{POC} and w_{sink} being taken as constant.

The downward flux of particles, F_{POC} ($\text{mol C m}^{-2} \text{s}^{-1}$), is simply given by

$$F_{\text{POC}}(z) = w_{\text{sink}}\{\text{POC}(z)\} = F_{\text{POC}}(z_0)e^{-(z-z_0)/z^*} \quad (5.31)$$

where $F_{\text{POC}}(z_0) = w_{\text{sink}}\{\text{POC}(z_0)\}$.

Particles associated with mineral material are denser, sink faster and reach a greater depth before complete respiration. Mineral ballast protects part of the organic matter and effectively reduces the respiration rate, λ_{POC} , and so increases the depth at which the organic material becomes regenerated, z^* . Particles originating in communities dominated by diatoms or coccolithophores have a higher sinking speed, w_{sink} , and deeper regeneration length scale, z^* , driven by the dense mineral components.

In reality, sinking particles are a mixture of accessible and mineral protected organic matter (see Fig. 5.20b, dashed and dotted lines).

illustrated in Fig. 5.21, where the scatterplot of inorganic nutrients is more or less aligned with the dashed lines reflecting the canonical Redfield ratios.

The concept of 'fixed' Redfield ratios is a useful device with which to develop simple frameworks to interpret the relationship of the carbon cycle and those of other elements. However, in addition to the variability in elemental ratios between and within phytoplankton species (Table 5.2), there is a

significant spread of ocean data points away from this canonical relationship in Fig. 5.21. Notably the slope of the nitrate-phosphate scatterplot is slightly shallower than 16, reflecting a global deficit of nitrogen relative to phosphorous compared to a Redfield balance.

Variations in the nutrient cycles lead to departures in the nutrient ratios from the canonical Redfield values. Next we consider the differences in the cycling of some key elements.

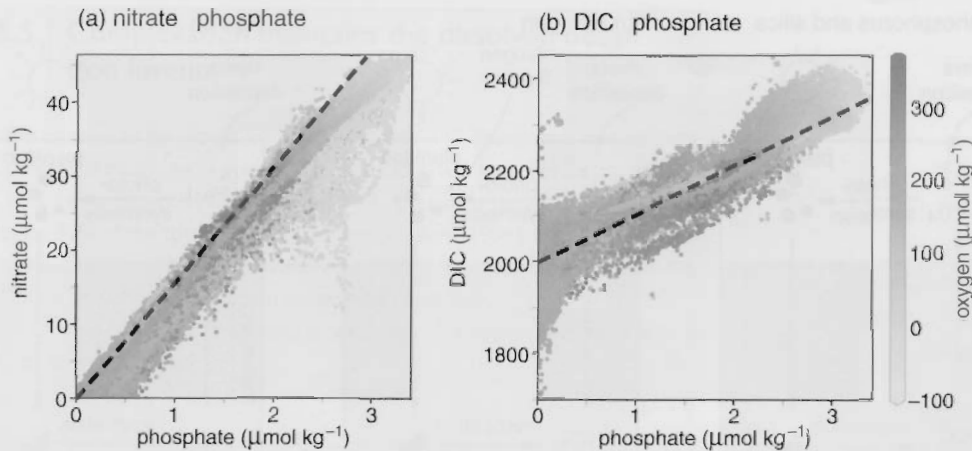


Figure 5.21 Relationships between observed concentrations of (a) nitrate and phosphate, and (b) dissolved inorganic carbon (DIC) and phosphate ($\mu\text{mol kg}^{-1}$) in the global ocean. Grey shading indicates the dissolved oxygen concentration ($\mu\text{mol kg}^{-1}$). The data reveal the close relationship between ocean nutrient ratios and those of 'average' marine plankton or Redfield ratios (dashed lines) of $\delta\text{DIC} : \text{NO}_3^- : \text{PO}_4^{3-} = 106 : 16 : 1$. δDIC is the difference in dissolved inorganic carbon from a reference value. Data from Key *et al.* (2004).

5.6.1 Contrasts in nutrient cycles

Nutrients are incorporated into organic matter in the surface ocean and regenerated in deeper waters. The global distributions of nutrients are primarily controlled by a combination of the biological cycling and physical transport and mixing processes. Circulation and biological export come into a global equilibrium over a few thousand years. Differences in the sources and sinks of the key elements, phosphorus, nitrogen, silica and iron, affect the phytoplankton community structure and cycling of organic matter, as illustrated schematically in Fig. 5.22:

- Phosphorus trickles into the ocean from rivers and atmospheric deposition, and is buried in sediments (Fig. 5.22a). These fluxes are small relative to the physical and biological transfers within the water column. Phosphorus has a lifetime of about 100 000 years in the ocean. Silicon also has riverine sources and a loss due to burial. It is utilised by some organisms to provide mineral structural material, which sinks and is redissolved, but more slowly than the remineralisation of most organic matter.
- Nitrogen likewise has sources from rivers and atmospheric deposition, but is also supplied to

the ocean through biological fixation of soluble nitrogen gas. Nitrogen is ultimately lost from the ocean in low oxygen waters and sediments through denitrification (Fig. 5.22b). In a low oxygen state, microbes use nitrate to provide the oxidising agent for organic matter, eventually returning nitrogen to gaseous form, which is lost from the ocean. Due to these additional sources and sinks, nitrogen has a lifetime on the order of 10 000 years in the ocean (Gruber, 2004), much shorter than that of phosphorus. The departure from Redfield ratio of nitrate and phosphate can be quantified by

$$\text{DIN}_{\text{xs}} = \text{NO}_3^- - 16\text{PO}_4^{3-} \quad (5.32)$$

(Hansell *et al.*, 2004), and the close variant, N^* which adds a constant (Gruber *et al.*, 1996). This tracer provides a clue as to the relative sizes of the sources and sinks of nitrogen to and from the ocean: higher values indicate an overall nitrogen supply to the ocean, such as from nitrogen fixation, while lower values represent an overall loss from the ocean, such as from denitrification; as illustrated in Fig. 5.23b.

- Iron is carried as windborne dust from the continents and deposited on the ocean, where a

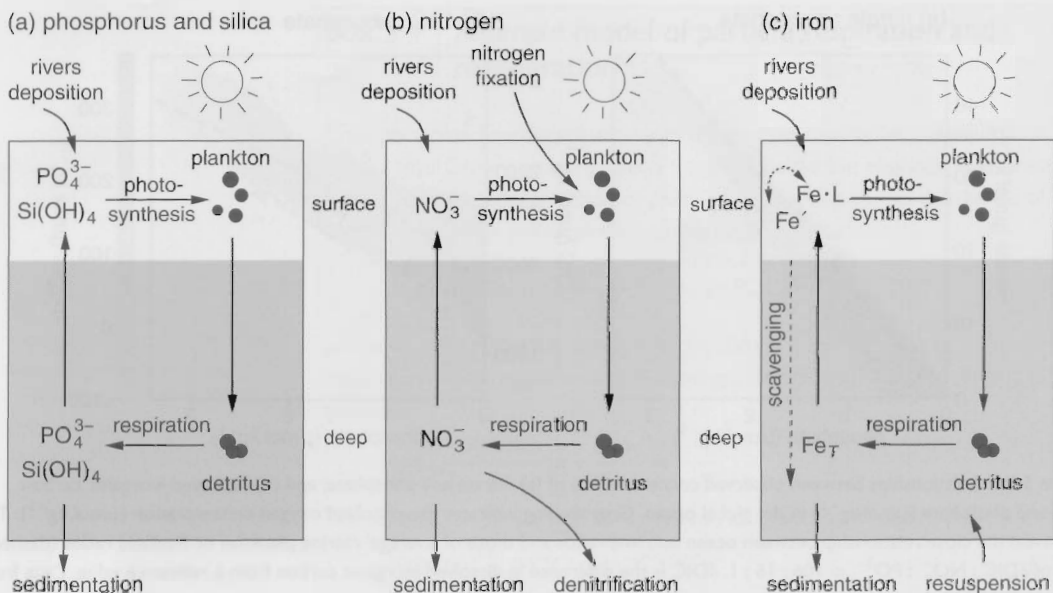


Figure 5.22 Contrasting global nutrient cycles for (a) phosphorus and silica, (b) nitrogen and (c) iron. In (a), phosphorus and silica pass into the ocean from rivers and atmospheric deposition and are buried in sediments. In (b), nitrogen is also fixed from nitrogen gas in the surface ocean and returned to gaseous form through denitrification in low oxygen waters and sediments. In (c), the total dissolved iron, Fe_T is made up of free iron, Fe^f and a complex form, $Fe \cdot L$, bound to a ligand. The free iron sticks to sinking particles and is quickly scavenged from the water column, leaving most of the dissolved iron in the complex form. Iron is supplied to the ocean through windborne dust from the continents, and released from sediments and hydrothermal vents. Adapted from a figure by F. Monteiro.

fraction enters the dissolved phase (e.g., Mahowald *et al.*, 2009). Iron is also released from sediments and hydrothermal vents. Dissolved iron is in a highly oxidised state which has extremely low solubility. Iron is incorporated into organic matter, exported and regenerated along with other elements. However, unlike nitrate and phosphate, dissolved iron has a very low solubility, sticks to sinking particles and is rapidly scavenged from the water column and lost to the sea floor (Fig. 5.22c). Nearly all of the dissolved iron is bound to organic ligands, molecules with appropriate binding sites (Johnson *et al.*, 1997), which provide some protection from scavenging (see Box 5.5). The concentration of dissolved iron is on the order of 1 nmol kg^{-1} in seawater. Iron is an essential nutrient for phytoplankton, playing a key role in light harvesting and nitrogen-fixing enzymes, but is a minor contributor to the mass of phytoplankton cells. The observed $Fe:C$ ratio varies widely from $1 \cdot 10^3$ to $1 \cdot 10^6$ (Boyd *et al.*, 2007). Iron has a very dynamic

cycle in the ocean, with an average lifetime on the order of 100 years (Bruland *et al.*, 1994).

The contrasting cycles of nitrogen, phosphorus, iron and silicon lead to subtle differences in the distributions of their dissolved inorganic forms, observed along a meridional section in the North Atlantic ocean, illustrated in Fig. 5.23. Nitrate is very depleted throughout the surface (Fig. 5.23a) and the nitracline is depressed by downwelling in the subtropics. Tropical upwelling fuels primary and export production, and leads to an accumulation of regenerated nitrate at a few hundred metres below the surface. The contrast between nitrate and phosphate, measured by DIN_{XS} (Fig. 5.23b), shows higher values to the north and a decline to the south. This signal reveals how the North Atlantic is a region of nitrogen fixation, sustained by the atmospheric deposition of iron-rich dust from the Sahara, which elevates the tropical surface iron concentration, even though nitrate is completely depleted (Fig. 5.23c), and

Box 5.5 Complexation maintains the dissolved ocean iron inventory

Iron in the ocean can be separated into particulate and dissolved forms, defined by the passage through an 0.4 μm filter. Total dissolved iron, Fe_T , is composed of free iron, Fe' , and a complexed form, $\text{Fe} \cdot \text{L}$, bound to organic ligands, which accounts for 99% of the total (Glehill and van den Berg, 1994). Free iron, Fe' has a very low solubility and is easily scavenged, and were it not for complexation, the concentration of iron would be even lower than observed.

Consider this complexation in more detail: free iron atoms, Fe' bind with a ligand, L, to form a complex $\text{Fe} \cdot \text{L}$,



The complex is held together by relatively weak intermolecular bonds and Fe' may eventually detach from $\text{Fe} \cdot \text{L}$, perhaps through thermal excitation or photodissociation. The rate of change of the concentration of free iron, $\{\text{Fe}'\}$ (mol m^{-3}), is represented in the forward and backward reactions of (5.33), which can also be described by the kinetic equation

$$\frac{d\{\text{Fe}'\}}{dt} = -k_f \{\text{Fe}'\}\{\text{L}\} + k_b \{\text{Fe} \cdot \text{L}\}, \quad (5.34)$$

where the rate of the forward reaction (leading to a loss of $\{\text{Fe}'\}$) is defined by k_f in s^{-1} (mol m^{-3}) $^{-1}$, and the rate of the reverse reaction is defined by k_b in s^{-1} . If a thermodynamic equilibrium is reached, then the rate at which the substrate binds with the ligand must equal the rate at which the substrate detaches from the complex, so that the concentrations of unbound substrate, ligand and complex become constant in time. Setting $d\{\text{Fe}'\}/dt = 0$ in (5.34), then the partitioning of iron is given by

$$\frac{\{\text{Fe} \cdot \text{L}\}}{\{\text{Fe}'\}\{\text{L}\}} = \frac{k_f}{k_b} = \beta_{\text{Fe}}. \quad (5.35)$$

This ratio is determined by the relative magnitude of the rate constants for the forward and backward reactions. For example, if the forward, binding reaction occurs with a much higher probability than the reverse, release reaction, $k_f \gg k_b$, then the equilibrium concentration of the complex is much higher than that of the substrate and free ligand. For iron binding to ligands in the ocean, β_{Fe} is very large (on the order of 10^{11} (mol kg^{-1}) $^{-1}$), so almost all of the dissolved iron is in complexed form. The concentration of iron-binding ligands in the ocean is about 1 nmol kg^{-1} or so, maintaining the dissolved iron concentration at a similar order. The sources, sinks and controls on the ligand concentration are still very unclear.

also has a signature of deeper regeneration. Silicic acid (Fig. 5.23d) is very depleted in the surface and its tropical, subsurface maximum is notably deeper than that of nitrate and iron, suggesting a slower rate of remineralisation relative to sinking organic matter, as well as being displaced southward, reflecting the effect of ocean transport and changes in the overlying phytoplankton community.

5.6.2 Modulation of regional productivity by iron: High Nitrate Low Chlorophyll regimes

Our first-order view is that primary production is restricted to the surface waters by light limitation and its basin-scale variations are controlled by the physical supply of macro-nutrients (nitrate and phosphate) to the euphotic layer. This view is modified by the

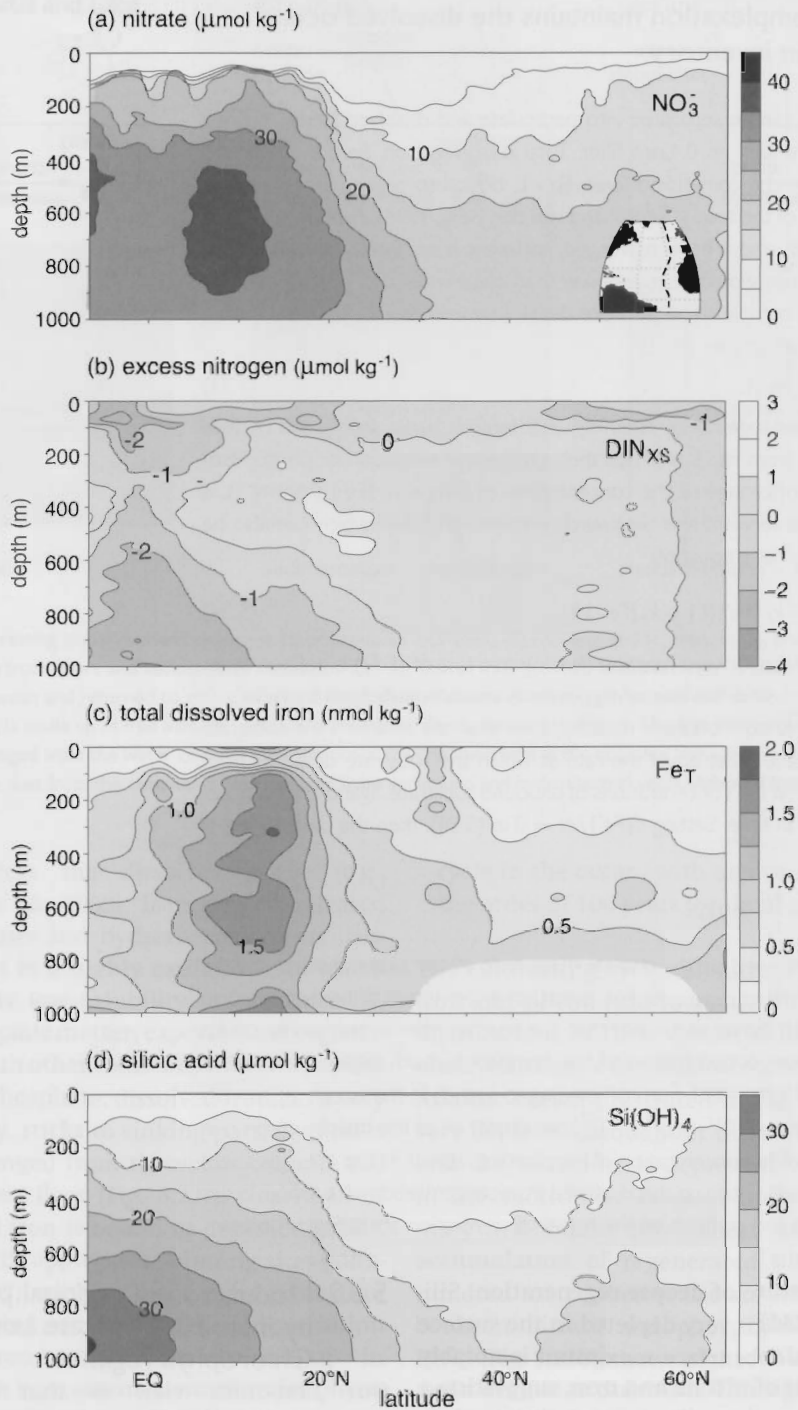


Figure 5.23 (a) Nitrate, NO_3^- ($\mu\text{mol kg}^{-1}$), (b) excess nitrogen $\text{DIN}_{\text{XS}} = \text{NO}_3^- - 16\text{PO}_4^{3-}$ ($\mu\text{mol kg}^{-1}$), (c) total dissolved iron, Fe_T (nmol kg^{-1}) and (d) silicic acid $\text{Si}(\text{OH})_4$ ($\mu\text{mol kg}^{-1}$) measured on a transect through the North Atlantic at approximately 20°W . (A&N CLIVAR Repeat Hydrography, 2003.)

essential role, but low abundance, of iron in the ocean.

In the mid and high latitudes of the North Atlantic, there is a striking seasonal phytoplankton bloom (Fig. 5.4) where phytoplankton rapidly grow and reduce nitrate concentrations to sub-micromolar concentrations in a few days. In contrast, in the Sub-Arctic Pacific, tropical Pacific and Southern Ocean, chlorophyll concentrations are never as intense, and micromolar concentrations of nitrate and phosphate persist in the surface waters all year round. In other words, the macro-nutrients are not completely utilised by the phytoplankton so primary and export production are not as vigorous in these areas as might be expected given the macro-nutrient concentrations; these regions are referred to as High Nitrate Low Chlorophyll (HNLC) regions.

Why does complete nutrient utilisation occur in the North Atlantic, but not in the Sub-Arctic Pacific or the Southern Ocean? A prevailing view is that the consumption of macro-nutrients is limited by the low availability of dissolved iron in the surface waters of the HNLC regions. In the deep ocean, free dissolved iron readily sticks to sinking particles and is scavenged from the water column rapidly. Dissolved iron concentrations are maintained at roughly nanomolar concentrations (10^{-9} mol kg $^{-1}$) through complexation with organic ligands (see Box 5.5). Upwelling waters have a deficit in dissolved iron relative to nitrate and phosphate, relative to the requirements for phytoplankton growth: they carry 30 μ mol kg $^{-1}$ NO $_3^-$ and 1 nmol kg $^{-1}$ of dissolved iron, which has an Fe : N ratio of 1 : 30 000, far short of the 1 : 2000 ratio in laboratory-grown phytoplankton cultures (Ho *et al.*, 2003). Thus, productivity in the subpolar and tropical regions of wind-driven upwelling is potentially limited by iron availability.

Part of this iron deficit can be compensated by atmospheric transport and deposition of iron-rich dust from the continents (Mahowald *et al.*, 2009). In regions like the North Atlantic, Saharan dust storms frequently deliver soluble, bio-available iron to the surface waters, elevating iron concentrations in the subtropics, in contrast to nitrate and silicic acid, and compensating for iron scavenging (see Fig. 5.23; also Measures *et al.*, 2008). In these iron-replete regions, the produc-

tion of iron-rich enzymes that enable nitrogen fixation, the associated signature of nitrogen fixation and enhanced iron supply over the tropical Atlantic can be seen in the increase in DIN $_{XS}$ in Fig. 5.23b and in later Fig. 11.14. In coastal waters, the release of dissolved iron from sediments also provides a significant source to the local surface ocean (Johnson *et al.*, 1999).

In contrast, in deep-water areas far from major continental dust sources, such as the Sub-Arctic Pacific and the Southern Ocean, the supply of iron from airborne and sedimentary sources is too weak to compensate for the deficit in upwelling waters, and limits the growth of phytoplankton. Martin and Fitzwater (1988) demonstrated this deficit by adding bio-available iron to water samples from the Sub-Arctic North Pacific, stimulating phytoplankton blooms. Subsequent open ocean iron-enrichment studies have shown similar responses in the water column (see earlier Fig. 3.19; Boyd *et al.*, 2007), supporting the view of iron limitation. However, efficient grazing or lack of light thick mixed layers caused by relatively may also play a role in limiting primary production in the HNLC regions.

5.7 Summary

Phytoplankton produce organic matter by photosynthesis in the surface ocean, converting electromagnetic energy into chemical energy. The organic matter, a fraction of which sinks into deeper waters, provides the source of energy for almost all living creatures in the ocean, including bacteria, zooplankton and fish. Phytoplankton gather energy from sunlight and the elements to build organic molecules from dissolved forms. The rate of production of organic matter by phytoplankton is thus controlled by the rate of supply of photons and essential nutrients into the cell, the rates of essential biochemical reactions, and the rate at which predation or viral infection control the phytoplankton population. In turn, nutrient and light availability to phytoplankton is regulated by ocean circulation and mixing processes. Biochemical reaction rates are affected by the temperature of the environment.

The elemental ratios in marine plankton reflect the collection of organic molecules which facilitate the functions of life. Though elemental ratios vary between species and with acclimation to the local environment, the average elemental composition of the plankton is $C:N:P:O_2 = 106:16:1:170$, referred to as the 'Redfield ratio'. These elemental ratios are broadly preserved in both production and respiration of organic matter. In turn, these ratios are reflected in the ratios of the inorganic nutrients within the water column.

Sunlight is rapidly absorbed in seawater so primary production is confined to the upper 200 m of the water column. Regional variations in primary production strongly mirror the pattern of upwelling of macro-nutrient enriched deeper waters. The vigour of production is reduced in some upwelling regimes because of a deficit of dissolved iron, relative to the requirements of phytoplankton. Global ocean primary production of organic carbon is estimated to be between 35 and 70 Pg C y⁻¹. Most of this organic matter is consumed and respired by zooplankton and bacteria mostly within the euphotic layer, but between 10 and 20 Pg C y⁻¹ passes into the deeper, dark ocean where organic carbon, too, is respired and returned to inorganic forms. Only a very small fraction of the exported organic carbon reaches the sea floor.

The effects of the ecosystem on the ocean carbon cycle are addressed further in Chapter 6, the role of seasonal variations in modulating production in Chapter 7, and how the interplay of biological transfers and physical transport determines nutrient and carbon distributions is discussed in Chapter 11.

5.8 Questions

Q5.1. How much carbon is in the microbes of the ocean?

Marine bacteria are typically on the order of $1 \mu\text{m}^3$ in volume and have a carbon content of about $50 \times 10^{-15} \text{ g C cell}^{-1}$. Bacteria are found throughout the whole water column with a population density of about $10^5 \text{ cells ml}^{-1}$. The smallest phytoplankton, *Prochlorococcus*, are of similar size and

carbon content, and there are also as many as $10^5 \text{ cells ml}^{-1}$ in the surface waters of the subtropical gyres, about half the ocean surface area, but restricted over the upper 250 m. Larger organisms typically occur at lower number densities, so most of the living organic carbon in the ocean is in the form of these smallest cells.

(a) Approximately how many bacterial cells are in the global ocean and how many *Prochlorococcus* cells? Assume that the volume of the global ocean is about $1.4 \times 10^{18} \text{ m}^3$.

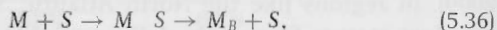
(b) Make an order of magnitude estimate of the amount of carbon in living microbes in the global ocean.

(c) If each *Prochlorococcus* cell divides once a day or less, provide an upper bound for the global rate of primary production (Pg C y⁻¹) by this organism?

Q5.2. Analogy of Michaelis-Menten type, two-stage process.

Consider a simple everyday example of a two-stage process involving children collecting marbles (inspired by Runge *et al.*, 2006). A teacher releases a large number of marbles, which spill across the floor in a gym, and asks the children to collect the marbles one by one and drop them into a single bucket. There are two stages, the first involves a child finding a single marble on the floor and the second involves the child carrying the marble to the bucket and dropping it in, which is then repeated.

We can write a pseudo-reaction to describe this game. To begin with, there are M uncollected marbles and S schoolchildren searching for an uncollected marble. Marbles being carried by the children are represented by M_S and marbles released into the bucket are represented by M_B . This process of collection and transfer of marbles is represented by



where the total number of schoolchildren, S_T , is given by the sum of the children searching for a marble, S , and those carrying a marble, M_S ,

$$S_T = S + M_S. \quad (5.37)$$

The rate of change of the number of uncollected marbles, M , is described by a loss, proportional to the number of uncollected marbles and the number of schoolchildren searching for a marble,

$$\frac{\partial M}{\partial t} = -k_{find}MS, \quad (5.38)$$

where the product $(k_{find}S)^{-1}$ represents the time for a single marble to be found and the product $(k_{find}M)^{-1}$ as the time for an individual child to find a marble.

(a) Assume that the rate of change of the number of marbles in the bucket, M_B , is given by the source, depending on the number of marbles being carried by a child divided by the time, \mathcal{T}_{drop} , to return the marble to the bucket and drop the marble in,

$$\frac{\partial M_B}{\partial t} = \frac{M}{\mathcal{T}_{drop}} S \quad (5.39)$$

Then show that the rate of change in the number of marbles being dropped into the bucket, M_B , is related to the number of uncollected marbles, M , by

$$\frac{\partial M_B}{\partial t} = \frac{S_T}{\mathcal{T}_{drop}} \frac{M}{(\mathcal{T}_{drop}k_{find})^{-1} + M} \quad (5.40)$$

(b) Consider the limit when there are very few marbles on the floor. What is the process limiting the rate of increase in the marbles being dropped in the bucket? How is the rate of change of M_B written in this limit?

(c) Now consider the opposing limit when there are a lot of marbles on the floor. What is the process limiting the rate of increase in the marbles being dropped in the bucket? How is the rate of change of M_B written in this limit?

Q5.3. Nutrient diffusion towards the cell.

Consider the down-gradient diffusion of nutrient molecules, \mathcal{N} towards a spherical cell of radius R . The transport or area-integrated flux towards the cell ($\text{mol s}^{-1} \text{cell}^{-2}$) through any sphere of radius $r > R$, can be described as

$$\int F(r)dA = 4\pi r^2\kappa \frac{\partial \mathcal{N}}{\partial r} \quad (5.41)$$

where κ is a molecular diffusivity ($\text{m}^2 \text{s}^{-1}$), $F(r)$ is the diffusive flux per unit area ($\text{mol s}^{-1} \text{m}^{-2}$) and

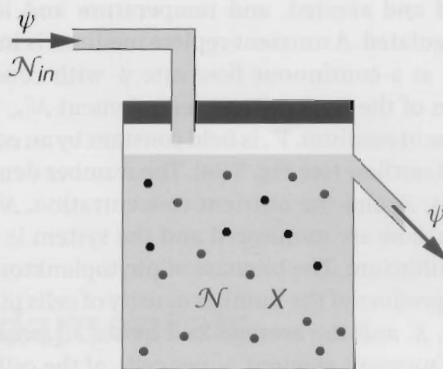


Figure 5.24 Schematic view of chemostat apparatus.

$\int dA$ is the surface area of the cell ($\text{m}^2 \text{cell}^{-1}$) taken to be a sphere of radius R .

Assume that a quasi-equilibrium state is reached in which the cell is acquiring nutrients at a constant rate and the transport of nutrient towards the cell through any sphere around the cell is also constant. By continuity, $\int F(R)dA$ is the rate of transport of nutrient into the cell which is facilitated by the cell-wall transporters.

(a) Derive an expression for the cell's rate of nutrient uptake in terms of R , $\mathcal{N}(R) = \mathcal{N}_0, \mathcal{N}_\infty$ and κ by re-arranging (5.41) and integrating from the radius R far away from the cell.

(b) Under what circumstances might the near-cell concentration of the nutrient become almost depleted such that $\mathcal{N}_0 \ll \mathcal{N}_\infty$?

(c) For the regime discussed in (b), if the average cellular content of \mathcal{N} is constant, Q_N (mol cell^{-1}), write a simple expression for the population growth rate, μ (s^{-1}) in terms of cell radius.

(d) If you initialised a batch culture study in the laboratory with two individual cells, one 5 microns in diameter and the other 50 microns, would the number density of the smaller or larger cells increase more rapidly?

Q5.4. Nutrient content and growth of phytoplankton.

The chemostat is an experimental apparatus used to study the physiology of phytoplankton and bacteria. The vessel is filled with a nutrient-replete medium (e.g., filtered seawater) and a seed population of the organism of interest. The vessel is

stirred and aerated, and temperature and light are regulated. A nutrient-replete medium is introduced at a continuous flow rate ψ with concentration of the limiting nutrient element \mathcal{N}_{in} . The volume of medium, V is held constant by an equal rate of outflow (see Fig. 5.24). The number density of cells, X , and the nutrient concentration, \mathcal{N} in the outflow are monitored and the system is run to equilibrium. The biomass of phytoplankton, B , is the product of the number density of cells in the vessel, X , and the average 'cell quota', $Q_{\mathcal{N}}$ (quantity of nutrient element \mathcal{N} per cell), of the cells in the vessel:

$$B = Q_{\mathcal{N}}X. \quad (5.42)$$

Conservation equations can be written for the nutrient,

$$\frac{d\mathcal{N}}{dt} = -\rho_{\mathcal{N}}X - D(\mathcal{N} - \mathcal{N}_{in}) \quad (5.43)$$

the biomass,

$$\frac{dB}{dt} = \rho_{\mathcal{N}}X - DB, \quad (5.44)$$

and the number density in the vessel,

$$\frac{dX}{dt} = \mu X - DX, \quad (5.45)$$

where the 'dilution rate', D , is determined by the flow rate and the volume of medium, $D = \psi/V$. The inflowing medium contains no phytoplankton, so that $X_{in} = 0$ and $B_{in} = 0$, whereas there is an input of the limiting nutrient, \mathcal{N}_{in} . The variables are: D (s^{-1}), the dilution rate; \mathcal{N} (mol m^{-3}), the concentration of the limiting nutrient in the vessel; $Q_{\mathcal{N}}$ (mol cell^{-1}), the 'cell quota' of element \mathcal{N} ; X (cell m^{-3}), the number density of cells in medium; V (m^3), the volume of medium in the vessel; $\rho_{\mathcal{N}}$ ($\text{mol cell}^{-1} s^{-1}$), the cellular uptake rate of dissolved nutrient element \mathcal{N} ; μ (s^{-1}), the exponential growth rate of population; and ψ ($\text{m}^3 s^{-1}$), the rate of inflow/outflow.

(a) Without measuring the composition of the cells directly, how would you estimate the

cell quota, $Q_{\mathcal{N}}$, of element \mathcal{N} in the cells at equilibrium?

(b) How would you control the experimental system to examine the relationship between growth rate, μ , and cell quota, $Q_{\mathcal{N}}$?

(c) Using a chemostat, Burmaster (1979) evaluated the relationship between exponential population growth rate and cell quota of phosphorus, Q_P under equilibrium conditions, as illustrated in Fig. 5.8. Why is the intercept with the x -axis not at $Q_P = 0$?

(d) The cell quota of phosphorus varies by an order of magnitude across the set of experiments. What underlying processes might this reflect? Why would a high cell quota be associated with higher growth rate?

(e) Speculate on which physical regimes a chemostat system might be a useful analogy in understanding how an oceanic phytoplankton population is controlled?

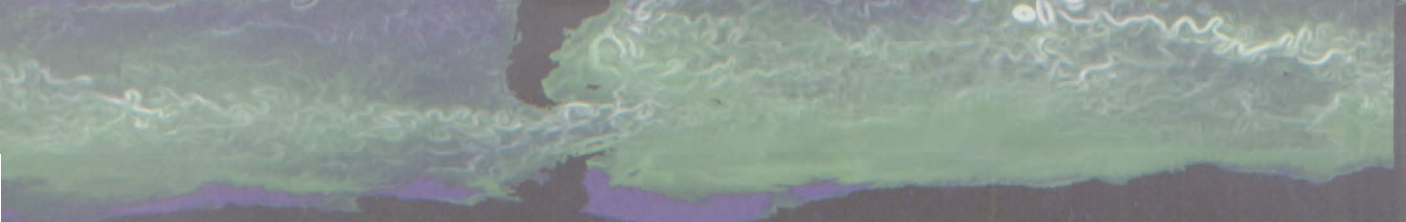
5.9 | Recommended reading

For a comprehensive, mechanistic description of the physiology of light harvesting and photosynthesis in marine phytoplankton, read P. G. Falkowski and J. Raven (1997). *Aquatic Photosynthesis*. Princeton, NJ: Princeton University Press.

An excellent, mechanistic discussion of how plankton live in their fluid environment is provided by T. Kjørboe (2009). *A Mechanistic Approach to Plankton Ecology*. Princeton, NJ: Princeton University Press.

An introductory overview of biological oceanography is provided by C. B. Miller (2004). *Biological Oceanography*. Malden, MA: Blackwell, 416pp.

A comprehensive review of nutrient and carbon cycles is provided by J. L. Sarmiento and N. Gruber (2006). *Ocean Biogeochemical Dynamics*. Princeton, NJ: Princeton University Press, 526pp.



The oceans play a crucial role in the climate system by redistributing heat and carbon across the planet through a complex interplay of physical, chemical and biological processes. This textbook for advanced undergraduate and graduate students presents a modern, multidisciplinary approach – essential for a complete understanding of ocean circulation and how it drives and controls marine biogeochemistry and biological productivity at a global scale.

Background chapters on ocean physics, chemistry and biology provide students from a variety of disciplines with a solid platform of knowledge to then examine the range of large-scale physical and dynamic phenomena that control the ocean carbon cycle and its interaction with the atmosphere. Throughout the text observational data are integrated with basic physical theory to address cutting-edge research questions in ocean biogeochemistry.

- Simple theoretical models, data plots and schematic illustrations are used to summarise key results and connect the physical theory to real observations.
- Advanced mathematics is provided in boxes and the appendix, where it can be drawn on as needed to put theory into practice.
- Numerous worked examples and homework exercises encourage students to develop first-hand experience and skills with real data and research problems.
- Further reading lists at the end of each chapter and a comprehensive glossary provide students and instructors with a complete learning package.

Praise for this book:

'This is an outstanding book, likely to become a standard text for those needing to know about both ocean physics and biogeochemistry...It will be widely adopted for upper-level undergraduate and graduate courses.' *Professor David Marshall, University of Oxford*

'The authors have carefully interwoven physical, biological and chemical fundamentals to achieve a modern approach to the study of the ocean's circulation and carbon cycle - creating the ideal course text for students and instructors alike.' *Professor Susan Lozier, Duke University*

'...thorough yet concise...excellent reading and provides a fresh approach that will be of immense value to future generations of students and new researchers.'
Professor Andreas Oschlies, IFM-GEOMAR, University of Kiel



www.cambridge.org/williamsandfollows

- All figures from the book
- Detailed solutions to exercises in the book
- Additional exercises and solutions for instructors
- Model animations linked to illustrations in the book

Cover design: OptaDesign

CAMBRIDGE
UNIVERSITY PRESS
www.cambridge.org

ISBN 978-0-521-84369-0



9 780521 843690 >